Dynamics, kinetics, and transport properties of the one-dimensional mass-disordered harmonic lattice

Vladimir N. Likhachev,* George A. Vinogradov,† and Tatyana Yu. Astakhova
N. M. Emanuel Institute of Biochemical Physics, Russian Academy of Sciences, ulica Kosygina 4, Moscow 119991 GSP-1, Russia

Andrey E. Yakovenko
Bauman Moscow State Technical University, 2-nd Baumanskaya Strasse, Moscow 105005, Russia
(Received 27 June 2005; revised manuscript received 8 September 2005; published 9 January 2006)

In the present paper we thoroughly investigated the dynamics, kinetics, and the transport properties of the one-dimensional (1D) mass-disordered lattice of harmonic oscillators with the number of particles $N \leqslant 5000$. The thermostat is simulated by the Langevin sources. Our method is adequate to any 1D lattice with linear equations of motion. Two accurate methods to calculate the temporal behavior of pair correlation functions were developed. The feature of the considered disordered model is an existence of localized states with great relaxation times τ to their stationary states. The exponential growth $\tau \propto \exp(N)$ is observed. A method which allows us to extend the range of computed relaxation times up to $\tau \simeq 10^{300}$ is suggested. The stationary state is unique. The thermal conduction $\varkappa$ has the nonmonotonic character versus N: for the number of particles $N < 300$ the thermal conduction increases as $\varkappa \propto \ln N$ and reaches the maximal value at $N \simeq 300$. At larger values the decreasing asymptotic is observed: $\varkappa \propto N^{-\alpha}$, and $\alpha \sim 0.27$. An influence of parameters on the calculated properties was analyzed. Mathematical problems associated with the computation of very large times of establishing the stationary states were extensively studied.

DOI: 10.1103/PhysRevE.73.016701 PACS number(s): 02.60.−x, 44.10.+i, 63.50.+x

I. INTRODUCTION

At present, many studies are focusing on the studies of statistical and transport properties of low-dimensional systems [1,2]. Besides the obvious achievements there are a few unresolved problems; e.g., does the unique stationary state really exist? If this state exists, then what is the relaxation time to its stationary state? What are the sufficient conditions for the observation of the finite value of the thermal conduction in low-dimensional systems?

The behavior of the thermal conduction $\varkappa$ vs. the number of particles N in the lattice and other parameters is also of great importance. Interest greatly increased after the pioneering work [3], where it was demonstrated that the thermal conduction diverges at the thermodynamical limit $(N \to \infty)$ for the lattice of nonlinear oscillators.

The diverging value of thermal conduction $\varkappa \propto N^{\alpha}$ with $0.17 \leqslant \alpha \leqslant 0.5$ was also observed for some model systems in the molecule dynamics (MD) simulations [4–7]. The final value of thermal conduction was obtained for other models [5,8–10], and, moreover, numerical simulations predict the "phase transition" from normal to diverging thermal conduction when temperature and/or parameters of the systems vary. However some of these results were criticized [11]. Theoretical estimations for α give values 2/5 [4,12,13] or 1/3 [14] depending on the chosen models.

Usually it is supposed that the nonintegrability is the necessary but not the sufficient condition for the final value of the thermal conduction in the one-dimensional (1D) systems [15]. It was demonstrated [4] that any 1D system with the acoustical branch of excitation should have an infinite value of $\varkappa$ in the low temperature limit.

Many model lattices with different potentials of interaction were investigated. Important qualitative and quantitative results were obtained, though controversial conclusions were made for the same model systems. These and associated problems are thoroughly considered in the recent reviews [1,2].

The existence of an anomalous energy diffusion in some systems [16,17] was also found, where $\sigma^2(t) = 2Dt^{\beta}$ $(0 < \beta \leqslant 2)$, and, moreover, the index β is related to α (in the dependence $\varkappa \propto N^{\alpha}$) by $\alpha = 2 - 2/\beta$. More complex systems were suggested and investigated for the heat rectification [18] and the controlling of the heat flow [19–21].

The 1D lattices are very useful prototypes for the analytical and numerical investigation of kinetic, dynamical, and transport properties of more complex and practically interesting systems such as carbon nanotubes (see, e.g., [22–29]).

The problem of the dynamics of the disordered lattices was formulated over 50 years ago by Dyson [30], who gave the general formulation of the problem. Dyson's problem was chosen for the detailed investigation, in the present paper, as this system meets some questions more or less common in the problem of thermal conduction in low-dimensional systems.

The structure of the paper is as follows. Section II describes the model formulates of the basic equations for the pair correlation functions. In our study we offer two methods for the accurate calculation of dynamics (vibrational spectrum), kinetics (relaxation of vibrational states to their stationary values), and transport properties (heat flow) of the

*Electronic address: vl@deom.chph.ras.ru
†Author to whom all correspondence should be addressed. Electronic address: gvin@deom.chph.ras.ru

mass-disordered lattice of the harmonic oscillators. These methods offer a clear and straightforward way to implement the necessary calculations of the values of interest, and have essential advantages in comparison with the MD simulations. Localized states and their role in the thermal conduction is considered in Sec. III. The results on the achievement of the unique stationary state, with corresponding relaxation times, the calculations of the stationary heat flow, and the thermal conduction are presented in the same section. An influence of the parameters values (choice of masses, "damping" γ in the Langevin forces, the different boundary conditions, and properties of the Langevin thermostat) are discussed in Sec. IV. Concluding remarks are made in Sec. V. Important mathematical details peculiar to the mass-disordered harmonic lattice are considered in the three Appendixes.

II. THE MODEL AND THE METHOD

We consider the one-dimensional (1D) lattice of N harmonic oscillators with distinct masses $m(i)$ and equal force constants. A paper where an analogous method was utilized is the work in [31], but for clarity, we give the more simple and advanced derivation of the main formulas.

The following dimensionless quadratic Hamiltonian

$$H = \frac{1}{2}\sum_{i=1}^{N} m(i)v^2(i) + \frac{1}{2}\sum_{i,j=1}^{N} x(i)U(i,j)x(j) \tag{1}$$

corresponds to the considered harmonic lattice. In (1) $v(i)$ and $x(i)$ are the velocity and displacement of the ith particle from its equilibrium position. The matrix $U(i,j)$ for the nearest neighbor interactions has the tridiagonal form

$$U(i,j) = \begin{cases} 2 & \text{if } j = i \\ -1 & \text{if } j = i \pm 1 \\ 0 & \text{in other cases.} \end{cases} \tag{2}$$

In (2) the fixed boundary conditions are assumed for the definiteness [for free boundary conditions $U(1,1) = U(N,N) = 1$]. The harmonic force constants in (1) are set to 1, $m_1 = 1$, and $m_2 = 1/2$, and are randomly and equaprobably distributed on the lattice.

For the evaluation of the thermal conduction it is reasonable to use the local formulation of the Fourier law [2]

$$J = -\varkappa \nabla T, \tag{3}$$

and both the temperature profile $T(i)$ and heat flow J should be determined. The stationary nonequilibrium conditions are fulfilled by applying the temperature difference at the lattice ends. [Note that the computation of thermal conduction in equilibrium conditions according to the Green-Kubo formalism [32] is unapplicable to harmonic lattices. The reason is that the normal modes do not interact in the harmonic lattices, and no "normal" behavior of the correlation function $\langle \mathbf{J}(0)\mathbf{J}(t)\rangle$ could exists.]

The Langevin thermostat is often used to prescribe definite temperatures to extreme particles in the lattice, and this thermostat allows us to make necessary calculus analytically.

We consider first the general case when the Langevin sources affect all particles in the lattice. In this assumption the linear equations of motion have an especially simple form

$$m(i)\ddot{x}(i) = [x(i-1) - 2x(i) + x(i+1)] + [-\gamma(i)v(i) + \xi(i)],$$

$$i = 1,2,\ldots,N, \tag{4}$$

where the expression in the first set of square brackets, is the harmonic interaction of ith particle with its nearest neighbors, and the fixed boundary conditions mean $x(0) = x(N+1) = 0$. The term $[-\gamma(i)v(i) + \xi(i)]$ is the Langevin force, where $\gamma(i)$ is the "damping" coefficient, and $\xi(i)$ is the random force. In the final expressions it will be easy to consider different partial cases by putting terms $\gamma(i) = \xi(i) = 0$ for some particles in the lattice.

Random forces obey standard relations (below for clarity, we introduce an explicit dependence on time for operators and functions)

$$\langle \xi(i;t_1)\xi(j;t_2)\rangle = 2\delta_{ij}\delta(t_1 - t_2)\gamma(i)T_{\mathrm{Lg}}(i), \tag{5}$$

where $T_{\mathrm{Lg}}(i)$ is an arbitrary temperature prescribed by the Langevin source to the ith particle.

It is convenient to substitute N the second order equations (4) by $2N$ of the first order equations

$$\dot{x}(i) = v(i),$$

$$\dot{v}(i) = \{[x(i-1) - 2x(i) + x(i+1)] + [-\gamma(i)v(i) + \xi(i)]\}/m(i). \tag{6}$$

Equations (6) provide the basis for the numerical MD simulation.

It is useful to utilize the more compact matrix notations. In order to do this we introduce the time-dependent vector of state,

$$\boldsymbol{q}(t) = \begin{pmatrix} \boldsymbol{v}(t) \\ \boldsymbol{x}(t) \end{pmatrix} = \{q(i;t)\}$$

$$= v(1;t), v(2;t), \ldots, v(N;t); x(1;t), x(2;t), \ldots, x(N;t) \tag{7}$$

and it is convenient to rescale the random forces

$$\tilde{\xi}(i;t) = \xi(i;t)/m(i). \tag{8}$$

Then system (6) can be rewritten as a matrix equation

$$\dot{\boldsymbol{q}}(t) = \hat{A}\boldsymbol{q}(t) + \begin{pmatrix} \tilde{\boldsymbol{\Xi}}(t) \\ \mathbf{0} \end{pmatrix}, \tag{9}$$

where $\tilde{\boldsymbol{\Xi}}(t) = \tilde{\xi}(1;t), \tilde{\xi}(2;t), \ldots, \tilde{\xi}(N;t)$—$N$ vector of random forces and $(2N \times 2N)$ matrix $\hat{A}$ does not depend on time and reads

$$\hat{A} = \begin{pmatrix} -\hat{M}^{-1}\hat{\Gamma} & -\hat{M}^{-1}\hat{U} \\ \hat{I} & \hat{0} \end{pmatrix}. \tag{10}$$

Matrix $M(i,j) = \delta_{ij}m(i)$ is the random diagonal matrix of particle masses and $\hat{M}^{-1}$—inverse matrix; $\Gamma(i,j) = \delta_{ij}\gamma(i)$ is the diagonal matrix of damping coefficients in the Langevin

forces. Matrix $\hat{U}$ is defined by (2). $\hat{I}$ and $\hat{0}$—unit and null matrices, correspondingly. Random matrix $\hat{A}$—non-Hermitian and its eigenvalues are complex values (see, e.g., review [33]).

Our goal is to find the time dependence of pair correlation functions

$$C(i,j;t) \equiv \langle q(i;t)q(j;t)\rangle, \quad i,j = 1,2,\ldots,2N, \tag{11}$$

where $q(i;t)$ is defined by (7).

There are two basic methods of averaging in (11). The first is to "take readings" from one "long" phase trajectory and to make necessary averaging at different time instants. This approach is suitable only for the stationary state. We use an alternative approach where the averaging over the final states at time t is performed for a set of "short" trajectories. The latter method is also suitable for the nonstationary states. It can be demonstrated that the results of both methods coincide in the limit $t \to \infty$ (ergodic hypothesis).

The correlation function (11) can have the sense of temperature, heat flow, and others. For instance, at time t the temperature and the heat flow through ith particle can be found as

$$T(i)/m(i) = \langle v^2(i;t)\rangle = C(i,i;t),$$

$$j(i;t) = \langle [x(i;t) - x(i+1;t)]v(i;t)\rangle = C(i,i+N;t) - C(i,i+N+1;t). \tag{12}$$

The formal solution of Eq. (9) (with the initial condition $\boldsymbol{q}(t=0)=0$, i.e., all particles are at rest) is

$$\boldsymbol{q}(t) = \int_0^t d\tau \sum_{p=1}^{N} \mathbf{W}^p(t-\tau)\xi(p;\tau), \tag{13}$$

where the superscript p numerates the Langevin sources, and $\hat{W}$ is the evolution operator satisfying the equation

$$\frac{dW^p(i;t)}{dt} = \sum_{m=1}^{2N} A(i,m)W^p(m;t), \quad W^p(i;t=0) = \delta_{ip}. \tag{14}$$

(The general case where $\boldsymbol{q} \neq 0$, i.e., $T_0 \neq 0$, will be considered below.)

Vector $\mathbf{W}^p(t)$ has the velocity and coordinate components

$$\boldsymbol{W}^p(t) = \begin{cases} \{V^p(i;t)\} & [\equiv W^p(i;t) \text{ if } i = 1,2,\ldots,N] \\ \{X^p(i;t)\} & [\equiv W^p(i;t) \text{ if } i = N+1, N+2,\ldots,2N]. \end{cases} \tag{15}$$

Being written in vector notation, Eq. (14) for the vector $\mathbf{W}^p(t)$ reads

$$\dot{\boldsymbol{X}}^p(t) = \boldsymbol{V}^p(t), \quad X^p(i;t=0) = 0,$$

$$\hat{M}\dot{\boldsymbol{V}}^p(t) = -\hat{U}\boldsymbol{X}^p(t) - \hat{\Gamma}\boldsymbol{V}^p(t), \quad V^p(i;t=0) = \delta_{ip}. \tag{16}$$

Every vector $\mathbf{W}^p(t)$ describes the evolution of the considered system with damping (but in the the absence of random forces). At the initial moment $t=0$ and all particles are at rest except one, pth, with the velocity equal to unity.

Write now [keeping in mind the definition (13)] the matrix of the correlation functions

$$C(i,j;t) \equiv \langle q(i;t)q(j;t)\rangle = \int_0^t \int d\tau_1 d\tau_2 \sum_{n,p=1}^{N} W^n(i;t-\tau_1)W^p(j;t-\tau_2) \times \langle \tilde{\xi}(n;\tau_1)\tilde{\xi}(p;\tau_2)\rangle. \tag{17}$$

Using the expressions (5) and (8) for correlators of random forces in the rhs of (17), we lastly get the desired expression for the correlation functions

$$C(i,j;t) = \sum_{p=1}^{N} \frac{2\gamma(p)T_{\mathrm{Lg}}(p)}{m^2(p)} \int_0^t d\tau W^p(i;\tau)W^p(j;\tau). \tag{18}$$

Our next goal is to construct and analyze the equations for $\boldsymbol{W}^p(t)$. The evolution equation

$$\dot{C}(i,j;t) = \hat{A}\hat{C} + \hat{C}\hat{A}^{+} + \hat{D}, \tag{19}$$

where

$$D(i,j) = \sum_{p=1}^{N} \frac{2\gamma(p)T_{\mathrm{Lg}}(p)}{m^2(p)} \delta_{ip}\delta_{jp} \tag{20}$$

is usually considered (see, e.g., [1,31]), and note that (19) is the equation for $\sim 2N^2$ variables.

Now we limit ourself by two Langevin particles with temperatures $T_{\mathrm{Lg}}(1)$ and $T_{\mathrm{Lg}}(N)$, and only two vectors $\boldsymbol{W}^1(t)$ and $\boldsymbol{W}^N(t)$ are necessary to calculate the correlation function (18). In this case expression (18) can be rewritten as

$$C(i,j;t) = \frac{2\gamma T_{\mathrm{Lg}}(1)}{m^2(1)} \int_0^t W^1(i;\tau)W^1(j;\tau)d\tau + \frac{2\gamma T_{\mathrm{Lg}}(N)}{m^2(N)} \int_0^t W^N(i;\tau)W^N(j;\tau)d\tau. \tag{21}$$

Below we shall demonstrate that even one Langevin particle is sufficient to obtain necessary physical results in the limit $t \to \infty$. Indeed, let us change temperatures of two extreme particles in the same manner: $T_{\mathrm{Lg}}(1) \to T_{\mathrm{Lg}}(1) + \Delta T$, $T_{\mathrm{Lg}}(N) \to T_{\mathrm{Lg}}(N) + \Delta T$. The change of the correlation function $\Delta C(i,j;t=\infty)$ in (21) will have the form of a correlator for equal temperatures ΔT at the lattice ends

$$\Delta C(i,j;t=\infty) = \frac{2\gamma\Delta T}{m^2(1)} \int_0^\infty W^1(i;\tau)W^1(j;\tau)d\tau + \frac{2\gamma\Delta T}{m^2(N)} \int_0^\infty W^N(i;\tau)W^N(j;\tau)d\tau, \tag{22}$$

and it is evident that the change in heat flow is equal to 0. Because of the addictiveness of correlation functions on temperatures of the Langevin particles [see (18)], one can (without the loss of generality), put $T_{\mathrm{Lg}}(N)=0$ and choose $\Delta T = -T_{\mathrm{Lg}}(N)$ for this purpose. Thus, all correlators (18) can be expressed through one vector $\mathbf{W}^1(t)$.

In a suggested approach only $2N$ entries of the vector $\boldsymbol{W}^1(t)$ are sufficient to calculate the correlation function (18) [but not $\sim 2N^2$ variables as in (19)]. One can perform the calculations at a fixed choice of temperatures $T_{\mathrm{Lg}}(1)=1$. The results for other temperatures can be easily obtained by the linear rescaling. Note that this is valid only for the harmonic systems.

At the usage of the MD simulation for one sample (by a "sample" we hereafter understand the unique choice of mass distribution in the lattice), it is necessary to numerically integrate many random trajectories defined by the different sequences of random forces to get the statistically reliable results. At the suggested approach, it is necessary to find only one trajectory [the time dependence of the vector $\boldsymbol{W}^1(t)$].

Below we describe two approaches to solve Eqs. (16).

A. "Direct" method (integration) for the calculation of correlation functions

One should numerically (by, e.g., Runge-Kutta method) solve the linear Cauchy problem (16) for vector $\mathbf{W}^1(t)$ of length $2N$ (below we omit the superscript "1" for clarity).

The system of Eqs. (16) can be complemented by the differential equations for any values of interest. For example, if temperature $T(i;t)$ and the heat flow $j(i;t)$ should be known, then the following ordinary differential equations [see (12)]:

$$\frac{dT(i;t)}{dt} = \frac{2\gamma(1)T_{\mathrm{Lg}}(1)}{m^2(1)} m(i)[V^1(i;t)]^2,$$

$$\frac{dj(i;t)}{dt} = \frac{2\gamma(1)T_{\mathrm{Lg}}(1)}{m^2(1)} m(i)[X^1(i-1;t) - X^1(i;t)]V^1(i;t) \tag{23}$$

should to be added to (16). This approach allows us to get all values at time t [upper limit of numerical integration in (16) and (23)]. But our main interest is to find the stationary values of the heat flow and temperature profile at $t \to \infty$.

Before describing the method, note an interesting fact observed at the numerical integration of systems (16) and (23): the heat flow at the right "cold" lattice end with $T_{\mathrm{Lg}}(1)=0$ reaches its stationary state much faster as compared with the left "hot" end with $T_{\mathrm{Lg}}(N)=1$ (see Fig. 1). This phenomenon has a simple explanation. The cold end just serves as a sink for the heat flow, while at the hot end the energy is consumed to the energy transport (thermal conduction) and to the excitation of vibrational states. The heat flows at the right and left ends coincide at the stationary state as it should be.

Thus, the computation of the heat flow is reasonable to perform at the cold end of the lattice. The algorithm for the computation of the heat flow by the direct numerical integration is the following: one gets few successive values (corresponding to ascending time instants) and approximates them by the power function $J(t)=J(\infty)-at^{-b}$, its asymptotic value being the approximation to the stationary state. The "sliding" approximation technique was utilized using the last five computed values. The criteria of reaching the true stationary state is the stabilization of the parameters of the approximating curve (triangles in Fig. 1). At the comparatively small times ($t \sim 10^5$) the heat flow reaches its stationary value in the lattice with $N=2000$, and the sliding method greatly increases the convergence.

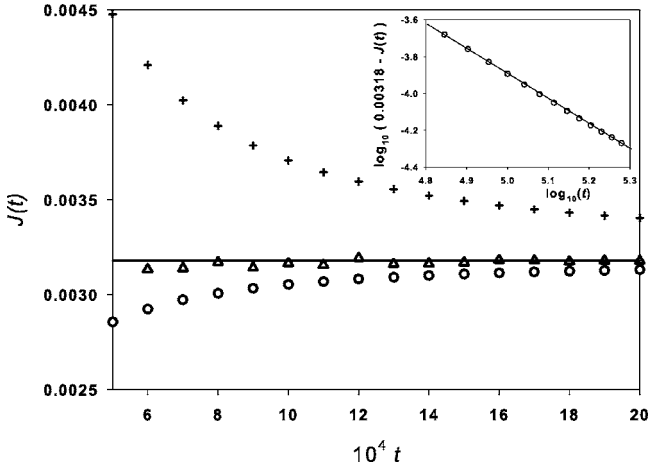

FIG. 1. The time dependence of the heat flows through the left (crosses) and right (circles) extreme particles for a random sample with $N=2000$. Triangles, sliding approximation calculated by five latest time instants (see the text). Horizontal solid line, the asymptotic value of thermal conduction $J(t=\infty)=0.03178$. The inset demonstrates the power law ($\log_{10}[J(\infty)-J(t)]$ vs t) for the right heat flow.

One of the advantages of the suggested "direct" approach of the computation of the heat flows consists in the necessity to solve the system of only $\sim 2N$, Eqs. (16) and (23), for only one Langevin particle. Namely, this approach was utilized at the calculations of thermal conductions of large lattices, and the results are presented below in Fig. 11.

B. "Matrix" method for the calculation of correlation functions

The other conventional approach to the solution of (18) consists of its transformation to the eigenvalue problem. The solution is searched as an expansion into a series in terms of eigenvalues and eigenfunctions of matrix $\hat{A}$ (10).

Let us consider the eigenvalue problem for the relaxing vibrational states (vibrations relax to their stationary states because of the damping in Langevin forces)

$$\hat{A}\boldsymbol{Q}_k = \lambda_k \boldsymbol{Q}_k, \tag{24}$$

where λ_k is the kth eigenvalue, and the eigenvector $\boldsymbol{Q}_k$ is evidently expressed through the (complex) amplitudes of the kth normal vibrational mode $\bar{\boldsymbol{x}}_k$: $\boldsymbol{Q}_k=\{\bar{\boldsymbol{v}}_k,\bar{\boldsymbol{x}}_k\}=\{\lambda_k\bar{\boldsymbol{x}}_k,\bar{\boldsymbol{x}}_k\}$, $\bar{\boldsymbol{x}}_k=\bar{x}_k(1),\bar{x}_k(2),\ldots,\bar{x}_k(N)$, and $k=1,2,\ldots,N$ (there are two complex conjugated values for each kth vibrational mode).

Equation (24) is rewritten in coordinate components for amplitudes of the kth vibrational state and has the form

$$-\hat{U}\bar{\boldsymbol{x}}_k - \lambda_k\hat{\Gamma}\bar{\boldsymbol{x}}_k = \lambda_k^2\hat{M}\bar{\boldsymbol{x}}_k, \tag{25}$$

and the complex value λ_k being the eigenvalue of operator $\hat{A}$ can be written as

$$\lambda_k = -1/\tau_k + i\omega_k, \tag{26}$$

where real τ_k and imaginary ω_k are the relaxation time to the stationary state and frequency, correspondingly. The values λ_k are not purely imaginary because the matrix $\hat{A}$ is non-Hermitian and its eigenvalues are complex in the general case. (The methods of solution of these matrix equations are considered in [34].)

Expanding the vector $\mathbf{W}(t)$ into a series in terms of eigenvectors $\boldsymbol{Q}_k$ one gets

$$W(i;t) = \sum_{k=1}^{2N} c_k Q_k(i)\exp(\lambda_k t), \quad i = 1,2,\ldots,2N. \tag{27}$$

The unknown expansion coefficients c_k can be determined from the linear system, obtained from (27) at $t=0$, and at the initial condition $W(i;t=0)=\delta_{i1}$

$$\delta_{i1} = \sum_{k=1}^{2N} c_k Q_k(i). \tag{28}$$

Substituting the expansion (27) into (18), one finally gets the expression for the pair correlation function

$$C(i,j;t) = \frac{2\gamma T_{\mathrm{Lg}}(1)}{m^2(1)} \sum_{k_1,k_2=1}^{2N} \frac{\exp[(\lambda_{k_1}+\lambda_{k_2})t]-1}{\lambda_{k_1}+\lambda_{k_2}} \times c_{k_1}c_{k_2}Q_{k_1}(i)Q_{k_2}(j), \tag{29}$$

and the time dependence is found only in the exponent.

The correlation function $C(i,j;t)$ allows us to get all physical values at an arbitrary time t. The most interesting stationary case ($t\to\infty$) is obtained by putting to zero the exponential phase multiplier and the fraction under a double summation in (29) is reduced to $-1/(\lambda_{k_1}+\lambda_{k_2})$. Recall that (29) is derived for only one Langevin particle with temperature $T_{\mathrm{Lg}}(1)$. The generalization for an arbitrary number of Langevin sources is obvious: there will appear the sum over the Langevin particles in accordance with the addictiveness of the results on their number and temperatures. One can check that (29) obeys Eqs. (18) and (20).

The comparison of the MD simulation with both direct and matrix methods demonstrates a very good accuracy: the mean standard deviation does not exceed 2% at statistical averaging over 100 MD trajectories. The better coincidence is expected with increasing the number of MD trajectories.

Expression (29) is formally analytically accurate; but it demands two numerical procedures: matrix diagonalization of $\hat{A}$ (10) and the solution of linear system (28). Thus the final accuracy of (29) is determined by the accuracy of the corresponding numerical operations. For the details of the calculation of eigenvalues and eigenvectors [Eq. (24)], and expansion coefficients [Eq. (28)], see Appendixes A and B.

III. RESULTS AND DISCUSSION

A. Localized states

An important property of the considered lattice is the existence of localized vibrational states with eigenfrequencies $\omega_k \sim 1$ and very small damping (very large relaxation times τ_k of kth vibrational states to their stationary values). Analogous localized states were discovered by Anderson [35] in the diffusion problem (see, also, review [36]). Just the computation of very large relaxation times is the main mathematical and computational problem of the considered harmonic disordered lattice.

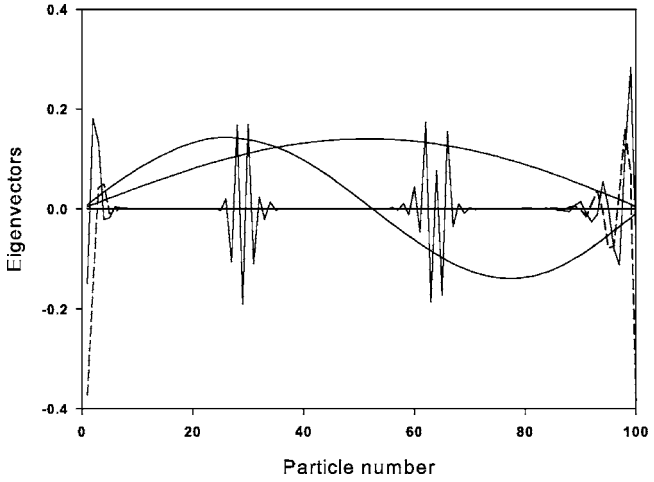

FIG. 2. Examples of vibrational states for a random sample with $N=100$. Shown are two vibrational states of three different types: mostly delocalized; mostly localized far from ends; and localized in the vicinity of lattice ends. Imaginary parts of eigenvectors are shown in dashed lines for the last type.

Different types of vibrational states give different contributions to the thermal conduction and temperature profile. As this takes place we consider the vibrational states in the disordered harmonic lattice.

As will be seen, the damping rate is determined by the boundary values of vibrational modes; therefore it is reasonable to classify the vibrational states by their amplitudes at the extreme left and right Langevin particles of the lattice.

Three types of vibrational states can be distinguished: first, long-wave acoustical vibrations with relatively large amplitudes at extreme particles; second, vibrational states localized far from both ends of the lattice, with negligible amplitudes at extreme particles; and third, vibrational modes localized in the vicinity of one end or the other end. These three types of vibrational modes are illustrated in Fig. 2.

For delocalized states and states localized far from the lattice ends their imaginary parts are much less compared to real parts and are not shown in Fig. 2. The opposite case is valid for the states localized close to one end or the other end; real and imaginary parts are comparable by modulus and are shown in Fig. 2.

The "map" of eigenvalues (frequencies) vs relaxation times is shown in Fig. 3. It turns out that the least relaxation times τ have the states localized close to one end or the other end of the lattice, and have the largest amplitudes at extreme Langevin particles. One can see that these states have comparable imaginary (ω) and real (τ) parts. Localized regions of points at small values of eigenvalues ω in Fig. 3 correspond to acoustical modes, and their frequencies behave as $\omega_k \propto k/N$.

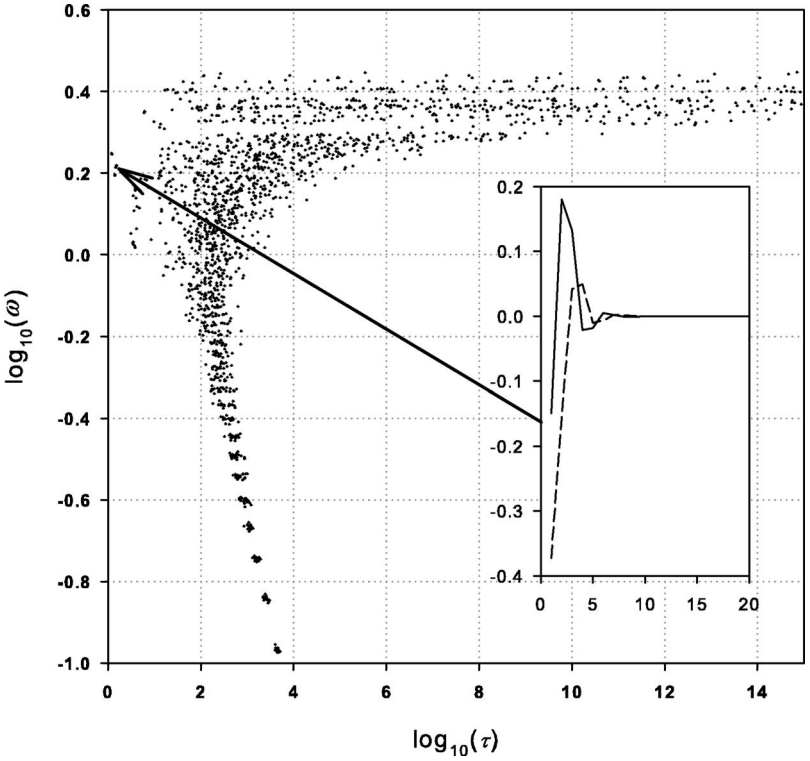

FIG. 3. The relationship between the eigenfrequencies ω and relaxation times τ for the lattice of $N=100$ particles, $M=20$ samples. The vibrational state localized at the left end is shown in the inset. Dashed line, the imaginary part of the eigenvector. The arrow shows the corresponding point in the map.

B. Maximal relaxation times to stationary states

It is convenient to determine the typical relaxation times of vibrational modes to their stationary states through the mean values of maximal relaxation times: for every sample with given N we determine $\tau_{\max}$; averaging over samples gives its mean value $\langle \tau_{\max} \rangle$.

The dependence of $\langle \log_{10} \tau_{\max} \rangle$ on the number of particles N in the lattice is shown in Fig. 4. One can see the linear dependence $\langle \log_{10} \tau_{\max} \rangle$ vs N, $\tau_{\max} \propto \exp(aN)$, where $a \approx 0.9$.

The dependence shown in Fig. 4 also allows us to determine the range of the number of particles N, where all physical values can be calculated exactly at achieving the true stationary state. The lower horizontal line for $t \lesssim 10^{14}$ limits $N \lesssim 50$, the upper horizontal line limits the range $N \lesssim 100$, where the relaxation times can be calculated exactly for $t \lesssim 10^{28}$ [see (A2) in Appendix A]. Note, that the accurate MD calculations are possible only for $t \lesssim 10^{9}$ and hence, $N \lesssim 25$.

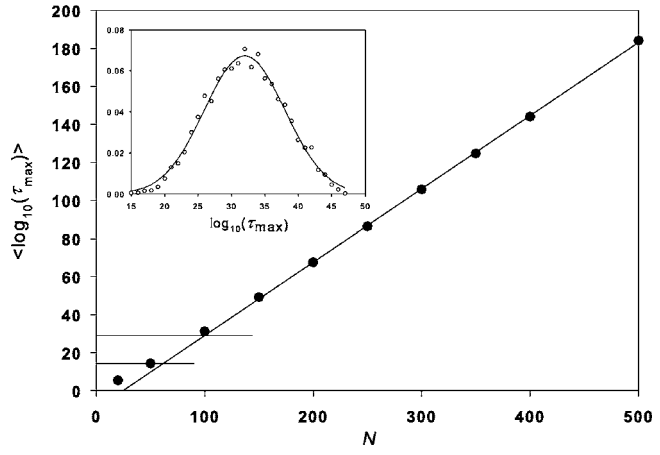

FIG. 4. The dependence of the logarithm of mean maximal relaxation times on the number of particles N in the lattice. Solid circles, calculated values; solid line, their linear approximation. Averaging over 1000 samples. Inset: The distribution function for relaxation times for $N=100$ (5000 samples) and its approximation by the normal distribution function.

Earlier [1] there was made an assumption that the relaxation times grow exponentially with N. This dependence is easily explained. If one of the localized state (having large relaxation time) is located approximately in the middle of the lattice, then the decreasing of its amplitude is exponential with the distance from the center of localization. According to (A2), relaxation times are proportional to squared amplitudes of vibrational states at extreme particles. Thus, the exponential dependence $\tau_{\max}$ vs N is also evident.

C. Kinetics of the stationary temperature profile establishing

The stationary temperature profile can be achieved when all vibrational modes reach their stationary values. But the mass-disordered harmonic lattice has localized vibrational states with very large relaxation times (see Fig. 4). The variation of the temperature profile vs time at different temperatures of thermostats calculated according to (29) is shown in Fig. 5. An extremely slow relaxation to the stationary temperature profile in the central region of the lattice is observed. Note that the temperatures in the vicinity of the lattice ends reach their stationary states rather soon.

In Appendix C we shall demonstrate how the results of the authors [37,38] for the stationary temperature profile can be obtained from (29) in the limit $\gamma \to 0$.

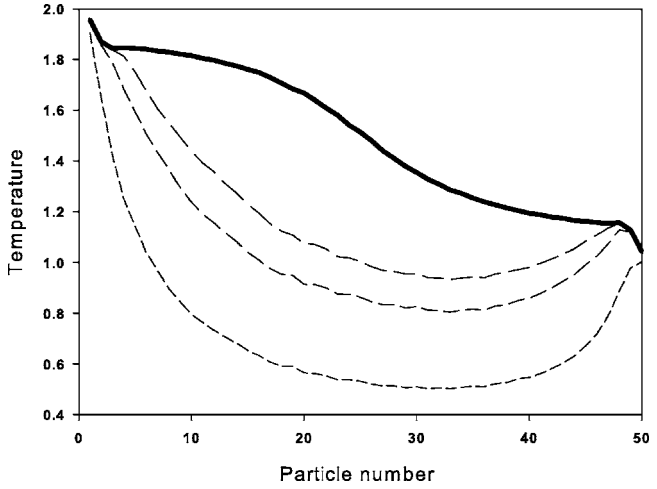

FIG. 5. The change of the temperature profile vs time t for the lattice of $N=50$ particles (averaging over $M=2000$ samples). The Langevin temperatures are $T_{\mathrm{Lg}}(1)=2$ and $T_{\mathrm{Lg}}(50)=1$. Times $t=10^2,10^3,10^4,t=\infty$ (thick solid line) for curves from down to up. The calculations by "direct" and "matrix" methods do coincide.

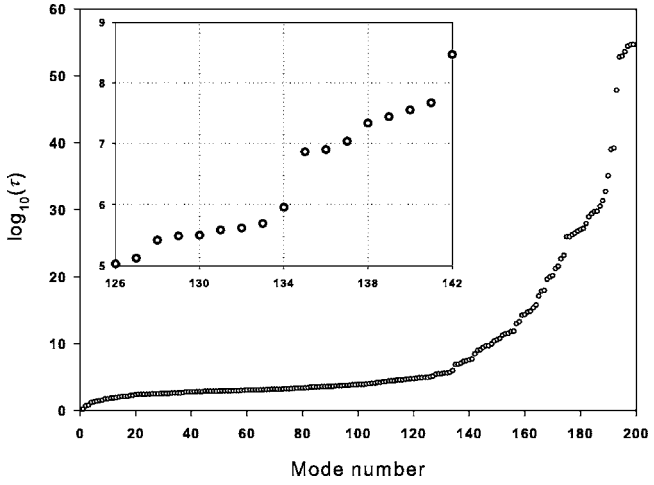

FIG. 6. The spectrum of relaxation times of a random sample with $N=200$. Inset: time range 10^5-10^8 is shown in a larger scale.

D. The uniqueness of the stationary state

The uniqueness of the stationary state in the case of general thermostats is still an open question [2]. But for the Langevin reservoirs this problem is solved in favor of the uniqueness of the stationary state. Indeed, it was demonstrated in [39] by an analysis of the Fokker-Plank equation and in [31,40], where an equation for the stationary correlation equations was considered.

The uniqueness of the stationary state is proved in our paper as we derived an accurate analytical expression obtained without any assumptions. Our results are nothing else than the solution of the linear Cauchy problem where no bifurcations can be observed, and consequently the solution is unique.

Earlier the question about the existence of the unique stationary state was discussed in [41] (the authors used the Nosé-Hoover thermostat). There two results were established: first, the temperature profiles are almost indistinguishable at times $t=10^6$ and 10^7 (initial temperature, $T_0=0.01$); second, the temperature profile depends sensitively on the initial conditions. The authors stated that the negligible difference in the temperature profiles at $t=10^6$ and 10^7 guarantees the existence of the stationary state. These results initiated some discussion (see [40,42]).

We have investigated the same problem but with the Langevin thermostat [43]. We found that this phenomenon (stabilization of the temperature profile in some time range) is also observed. We used the same parameters of the model as in [41]: number and masses of the particles, boundary temperatures, but slightly changed times—5×10^5 and 5×10^6. A random sample (mass distribution of particles with masses 1 and 1/2) was used. The difference in the used initial temperatures ($T_0=0$ in our work and $T_0=0.01$ in [41]) is negligible.

We have supposed that the temporal deceleration establishing the temperature profile is observed in the time range where there is a gap in the spectrum of relaxation times. This spectrum is shown in Fig. 6. One can see that the gap in the spectrum does really exist in the time range of interest (from $t=5\times10^5$ to $t=5\times10^6$).

The temperature profiles are shown in Fig. 7 and they are almost indistinguishable at times $t=5\times10^5$ and $t=5\times10^6$ (compare with Fig. 4(a) in [41]). Time is necessary to achieve the stationary state t_{st} for the mass-disordered harmonic lattice with $N=200$ many orders of magnitude greater, as is achieved in MD simulations and $t_{\mathrm{st}}\sim10^{50}$. Thus the "stabilization" of the temperature profile in some time range does not guarantee the existence of the stationary state, at least with the Langevin thermostat.

We considered next the case when the initial state was chosen from the Gibbs distribution corresponding to the initial temperature $T_0=3$, as in [41]. The Gibbs equilibrium distribution was generated by applying the Langevin sources with $T=3$ to all particles of the lattice. It was checked that time $t=10^2$ (at $\gamma=1$) is enough to establish the true stationary state.

To consider the evolution of the system, starting from the initial states with $\boldsymbol{q}_0\neq\mathbf{0}$ ($T_0\neq0$), we have to generalize our expressions for the correlation functions of Sec. II. This can be easily done; one should add the term

$$\delta C(i,j;t)=\boldsymbol{q}_0(i;t)\boldsymbol{q}_0(j;t) \tag{30}$$

to the rhs of all expressions for the correlation functions in Sec. II. The vector $\boldsymbol{q}_0$ satisfies the equation

$$\dot{\boldsymbol{q}}=\hat{A}\boldsymbol{q} \text{ where } \boldsymbol{q}_0(t=0)=\boldsymbol{q}_0\neq\mathbf{0}. \tag{31}$$

In the case of initial temperature $T=3$, it is necessary to average an expression $\boldsymbol{q}_0(i;t)\boldsymbol{q}_0(j;t)$ over the Gibbs distribution of initial vectors $\boldsymbol{q}_0$. The final expression for the additive to the correlation functions (31) reads

$$\delta\langle C(i,j;t)\rangle=\langle\boldsymbol{q}_0(i;t)\boldsymbol{q}_0(j;t)\rangle\big|_{\boldsymbol{q}_0}. \tag{32}$$

The additives to temperatures are $\delta T(i;t)=m(i)\langle\delta C(i,i;t)\rangle=m(i)\langle\boldsymbol{q}^2(i;t)\rangle\big|_{\boldsymbol{q}_0}$ and are shown in Fig. 8.

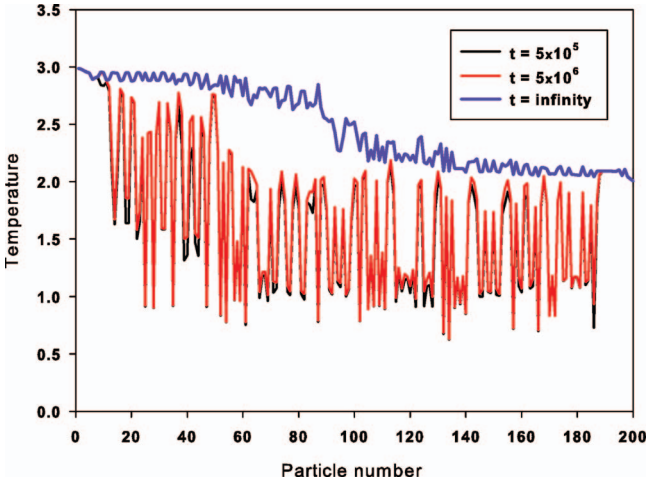

FIG. 7. (Color) The temperature profiles at times $t=5\times10^5$ and $t=5\times10^6$. Upper (blue) solid line, true stationary temperature profile at $t=\infty$. The sample is the same as in Fig. 6. $T_{\mathrm{Lg}}(1)=3$ and $T_{\mathrm{Lg}}(200)=2$. To distinguish the two almost coinciding curves, the colored curves are used.

The final additions to the temperatures in Fig. 8 will be $T(i;t=\infty)=0$, $i=1,2,\ldots,N$. Indeed, the temperatures in the vicinity of both ends of the lattice are practically equal to zero. It means that the modes with the least relaxation times just relaxed to their zeros stationary states at $t>5\times10^5$.

The summation of temperature profiles in Figs. 7 and 8 gives the desired temperature profile at times $t=5\times10^5$ and $t=5\times10^6$ and at the initial temperature $T_0=3$. The result is shown in Fig. 9 (compare with Fig. 4(a) in [41]). It is apparent that at $t\to\infty$ the temperatures will have the values shown in Fig. 7 as it is the unique stationary state at $t\to\infty$.

E. Calculation of the heat flow

For the computation of the thermal conduction we use an expression for the stationary value of heat flow combining (12) and (29)

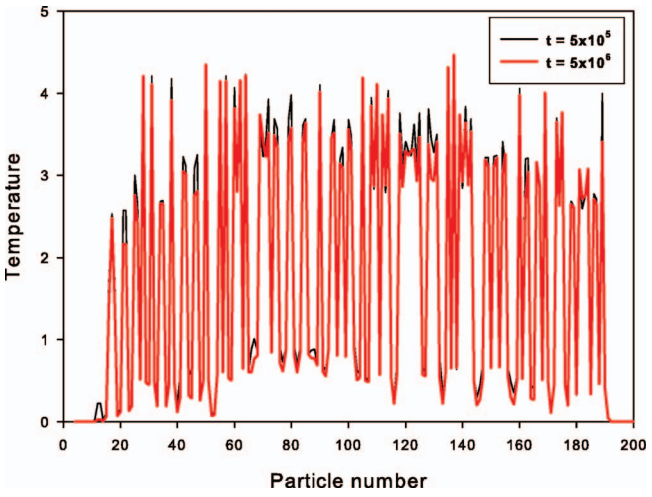

FIG. 8. (Color) The temperature profiles at times $t=5\times10^5$ and $t=5\times10^6$. Initial conditions at $t=0$, the Gibbs distribution at $T_0=3$. Averaging over 2000 initial vectors of state $\boldsymbol{q}_0$. The sample is the same as in Fig. 6.

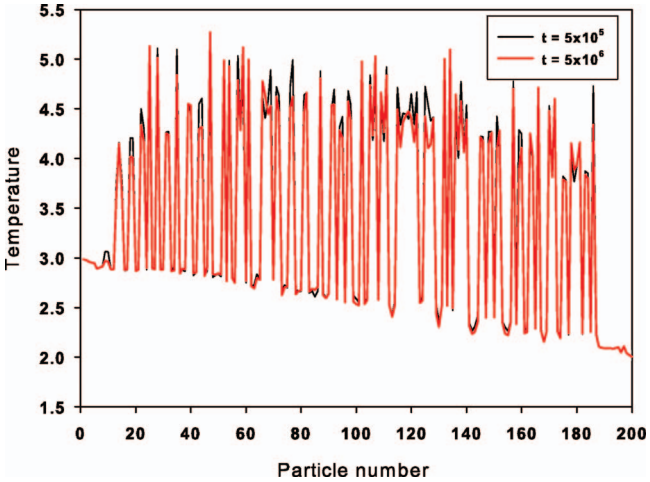

FIG. 9. (Color) Temperature profiles at $t=5\times10^5$ and $t=5\times10^6$ and the initial temperature $T_0=3$. The sample is the same as in Fig. 6. $T_{\mathrm{Lg}}(1)=3$ and $T_{\mathrm{Lg}}(1)=2$.

$$j(i;t=\infty)=\frac{2\gamma T_{\mathrm{Lg}}(1)}{m^2(1)}\sum_{k_1,k_2=1}^{2N}\frac{c_{k_1}c_{k_2}}{\lambda_{k_1}+\lambda_{k_2}}\times[X_{k_1}(i)-X_{k_1}(i+1)]V_{k_2}(i+1). \tag{33}$$

We also utilize two other well known definitions for the calculation of the stationary heat flow

$$J(t=\infty)=\begin{cases}\gamma[(T_{\mathrm{Lg}}(1)-T(1;t=\infty)]/m(1) & \text{for the first particle}\\ \gamma T(N;t=\infty)/m(N) & \text{for the } N\text{th particle},\end{cases} \tag{34}$$

where $T(1;t=\infty)$ and $T(N;t=\infty)$ stand for actual stationary temperatures of the first and Nth particles. The coincidence of values of heat flows obtained according to (33) and (34) served the additional criterium of the accuracy of the computations of the heat flow.

F. Contribution of different types of vibrational states to thermal conduction

An existence of three types of vibrational states was assumed above. Questions arose about their contributions to thermal conduction and other properties of the mass-disordered harmonic lattice.

Acoustical vibrations obviously give the main contribution to the thermal conduction. Actually, left Langevin particles (having higher temperature) excite acoustical modes (because of nonzero amplitude at this particle) and carriy the energy to the right particle, thus maintaining the thermal conduction. The contribution of vibrational states localized in the lattice center is negligible as their coupling with thermostat is very small.

Thus, acoustic delocalized states contribute to thermal conduction, stationary temperature profile, and heat capacity. Modes localized in the center do not participate in thermal conduction at all, but in the limit $t\to\infty$ contribute only to

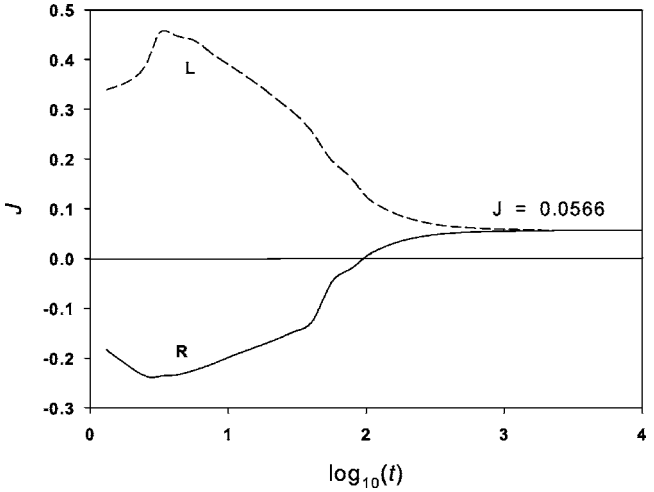

FIG. 10. The dependence of the heat flows J vs time for the lattice with $N=50$. L, the heat flow through the left end of the lattice; R, the same for right end. Averaging over $M=2000$ samples. The value of the stationary heat flow $J(t=\infty)=0.0566$ is also shown. The langevin temperatures are $T_{\mathrm{Lg}}(1)=2$ and $T_{\mathrm{Lg}}(50)=1$.

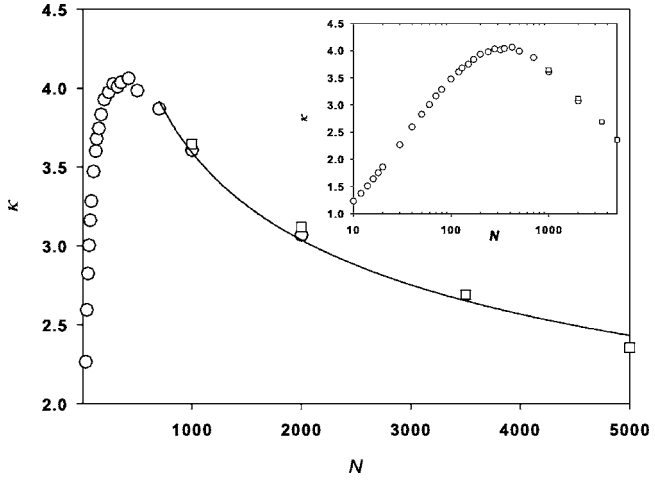

FIG. 11. The dependence of thermal conduction on the lattice length N ($10 \leqslant N \leqslant 5000$). Empty circles, calculation by the "matrix" method. Empty squares, "direct" integration. Solid line, approximation $\varkappa \propto N^{-\alpha}$) for $N>500$. Inset, the same dependence in semilogarithmic coordinates. The dependence $\varkappa \propto \ln N$ is obvious for $N \lesssim 300$.

temperature profile and heat capacity. Modes localized close to the lattice ends behave analogously, differing in a faster contribution to heat capacity and temperature profile.

The time dependence of the heat flow calculated in accordance with (33) is shown in Fig. 10. In spite of very large relaxation times (for the considered length $N=50\langle\tau_{\max}\rangle \sim 10^{14}$, see Fig. 4), the heat flow reaches its stationary state rather soon (at $t<10^4$).

All these are of concern in the calculation of thermal conduction. Actually it is not necessary to wait when the system reaches its true stationary state (see Fig. 5, where at $t \sim 10^4$ the temperature profile is very far from the stationary state) to calculate the thermal conduction.

Below we shall use the Fourier law in its integral formulation

$$J = \varkappa \frac{T_{\mathrm{Lg}}(1) - T_{\mathrm{Lg}}(N)}{N}, \tag{35}$$

and the accuracy of approximation (35) increases with the growth of the number of particles in the lattice. We calculated the coefficient of thermal conduction $\varkappa$ just according to (35). All localized states with relaxation times with $\tau \geqslant 10^6$ were excluded from consideration as their contribution to thermal conduction is negligible.

The dependence of $\varkappa$ vs the number N of particles in the lattice is shown in Fig. 11. One can see the nonmonotonic behavior of $\varkappa$: it has a maximal value at $N \approx 300$. At smaller values of N thermal conduction $\varkappa \propto \ln N$. For larger values the behavior changes qualitatively and the thermal conduction obeys the dependence $\varkappa \sim N^{-\alpha}$ with $\alpha=0.27$, i.e., the thermal conduction converges to zero in the thermodynamical limit. Recall that the following model is considered: a harmonic lattice with random distribution of masses $m_1=1$ and $m_2=1/2$; heat bath—one Langevin particle with $T_{\mathrm{Lg}}(1)=1$. The calculation was made by two methods—"direct" and "matrix." The role of parameters choice on thermal conduction will be considered in the next section.

A question was raised—is the heat flow a self-averaging value in the thermodynamical limit or not? (See Fig. 18 in [1].) The answer for this question is given by the value

$$S[J(N)] = \sigma_{J(N)}/\langle J(N)\rangle, \quad \langle J(N)\rangle = M^{-1}\sum_{i=1}^{M} J_i(N), \tag{36}$$

where $\sigma^2_{J(N)}$ is the standard deviation for the heat flow; M is the number of samples. If $S[J(N)] \to 0$ in the thermodynamical limit if J is the self-averaging value.

The value $S[J(N)]$ for the heat flow is shown in Fig. 12. It

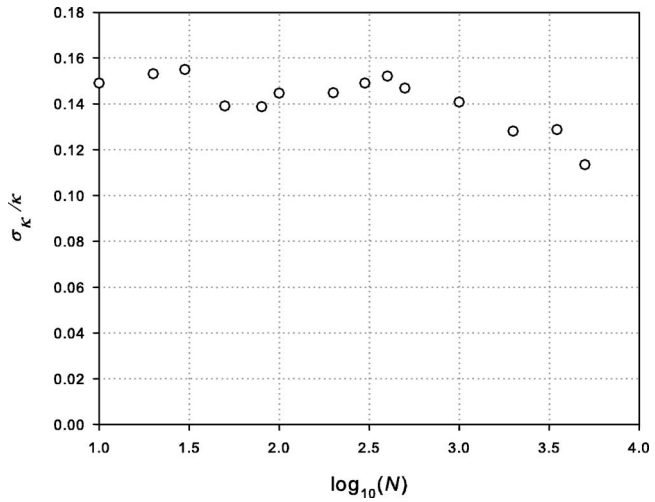

FIG. 12. The dependence of self-averaging characteristic $S=\sigma_\kappa/\kappa$ defined according to (36) on the number of particles N in the lattice. Averaging over $M=200$ samples.

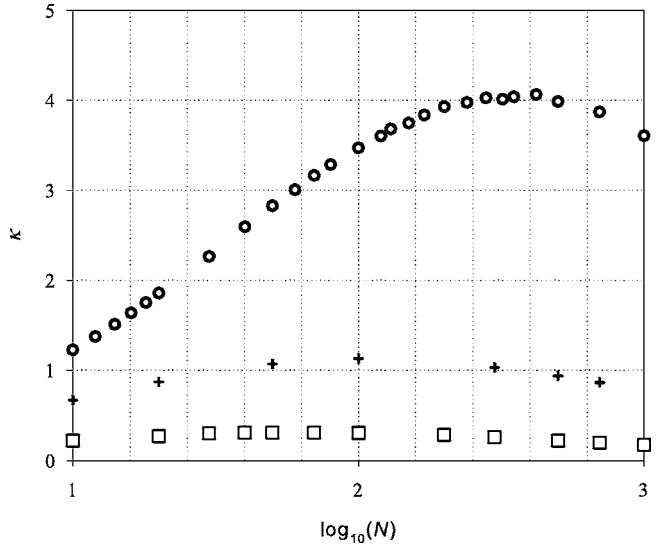

FIG. 13. Computed dependencies of thermal conduction vs lattice length N ($N \leqslant 1000$) at different relation of masses. $m_1=1$ in all cases. Circles, $m_2=1/2$ (the same as in Fig. 11); crosses, $m_2=1/5$; squares, $m_2=5$.

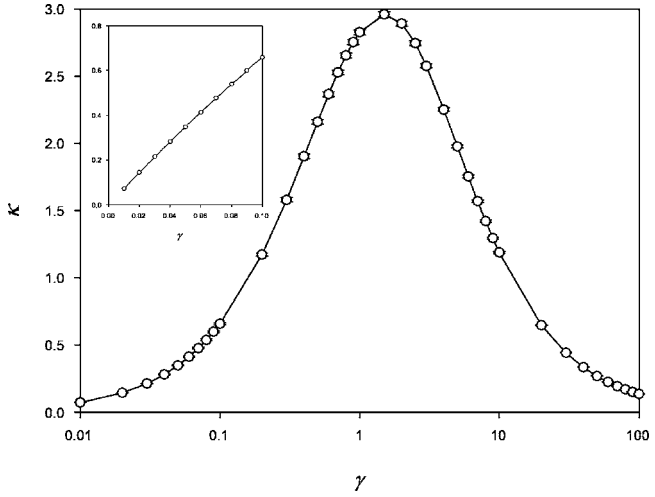

FIG. 14. The dependence of the thermal conduction on the value of damping parameter γ in the Langevin sources for the lattice with $N=50$ particles. Averaging over $M=5000$ samples. Inset: the linear dependence of $\varkappa$ vs γ at small values of $\gamma(0.01 \leqslant \gamma \leqslant 0.1)$.

is unlikely, according to Fig. 12, that the heat flow is the self-averaging value.

There could be made a "natural" assumption that the problems associated with the computation of vibrational mode with extremely large relaxation times can be avoided if weak fictitious damping is introduced for nonLangevenian particles in the lattice, analogous to that done in [31]. It is expected that in this case the lattice rather quickly achieves its stationary state and all necessary results can be obtained with much less computational effort. But we have shown that this idea fails, and results will be published elsewhere.

IV. AN INFLUENCE OF PARAMETERS VALUES ON THE PROPERTIES OF THE MODEL

All results described above were obtained at the following fixed choice of parameters: (i) uniform and random distribution of masses $m_1=1$ and $m_1=1/2$ in the lattice; (ii) fixed boundary conditions and only one (or two) extreme particles as Langevin sources; (iii) in Langevin sources ($F_{\mathrm{Lg}}=\xi-\gamma v$) they were set $\gamma=1$; (iv) the lattice does not interact with its surrounding. The natural question arises: How do the parameters' choice influence the quantitative, and, probably, qualitative behavior of thermal conduction? In this section we discuss these problems in more details.

A. Choice of masses

Other values of masses influence the results only qualitatively (see Fig. 13). The greater the mass relation, the less the value of thermal conduction. But in the limit $m_1/m_2 \to 1$ one should get the known dependence $\varkappa \propto N$ [1].

B. Parameter γ in Langevin forces

It was supposed [1] that the dependence of thermal conduction on γ has the asymptotics $J(\gamma) \to 0$ at $\gamma \to 0$ and $\gamma \to \infty$. Our results are in qualitative agreement with this suggestion. The dependence of the thermal conduction vs parameter γ changed by four orders of magnitude is shown in Fig. 14.

C. Influence of substrate

Inclusion of the interaction with a substrate is reflected in an extra term in (1)

$$H=\frac{1}{2}\sum_{i=1}^{N} m(i)v^2(i)+\frac{1}{2}\sum_{i,j=1}^{N} x(i)U(i,j)x(j)+\sum_{i=1}^{N} g(i)x(i), \tag{37}$$

and $g(i)$, is the parameter of interaction (on-site potential) depending on the particle number. Without loss of generality one can set $g(i)=g=\mathrm{const}$ and the randomness included in matrix $\hat{U}$. The addition of an interaction with the ubstrate changes the behavior qualitatively: the model becomes momentum nonconserving. Models of this type are known as having zero thermal conduction in the thermodynamical limit.

The dependence $\varkappa$ vs the lattice length N at different values of parameter g is shown in Fig. 15. The dependence obeys the exponential law $\varkappa \propto \exp(-bN)$, and the growth of parameter g results in an increase of index b. It means that the considered model with the on-site potential is the ideal thermal insulator in the thermodynamical limit.

D. Role of boundary conditions

In contrast to fixed boundaries where the dependence $\varkappa \propto 1/\sqrt{N}$ is expected, the diverging character $\varkappa \propto \sqrt{N}$ is valid for free boundaries [1].

At the analysis of the influence of the boundary conditions we have changed the force constant of interaction k of the interaction between the "wall" and the first and Nth par-

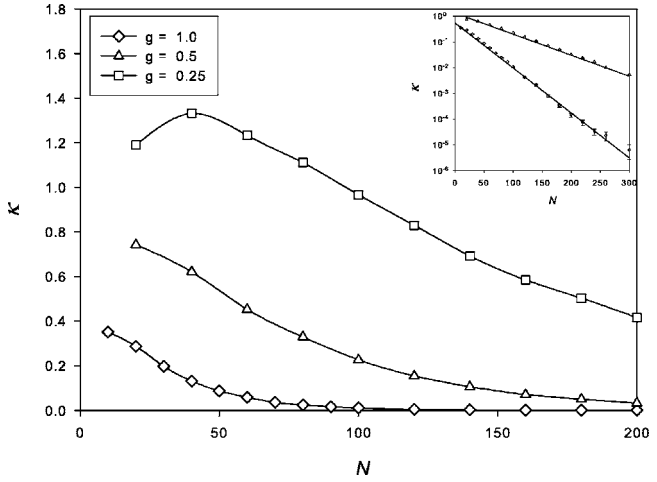

FIG. 15. The dependence of thermal conduction on the parameter g ($g=0.25, 0.5, 1.0$). Averaging over $M=5000$ samples. Inset: the same dependence in semilogarithmic coordinates ($\log_{10}\kappa$ vs N for $g=0.5$ and $g=0.25$).

ticles, i.e., we set $U(1,1)=U(N,N)=1+k$ in (2), and $k=0$ corresponds to free boundaries.

The dependence of $\varkappa$ on force constant k in the range $0\leqslant k\leqslant 10$ is shown in Fig. 16. An exponential decrease of $\varkappa$ with the increase of parameter k is found.

The dependence of thermal conduction $\varkappa$ vs the number of particles for the case of $k=0$ is shown in Fig. 17. This dependence obeys the predicted law $\varkappa\propto\sqrt{N}$ [1] with very good accuracy.

E. Number of Langevin particles and value of γ

The model considered above is nonphysical in the sense that the results are extremely sensitive to the choice of parameters of the heat reservoir (see Fig. 14 where the dependence on parameter γ is obvious).

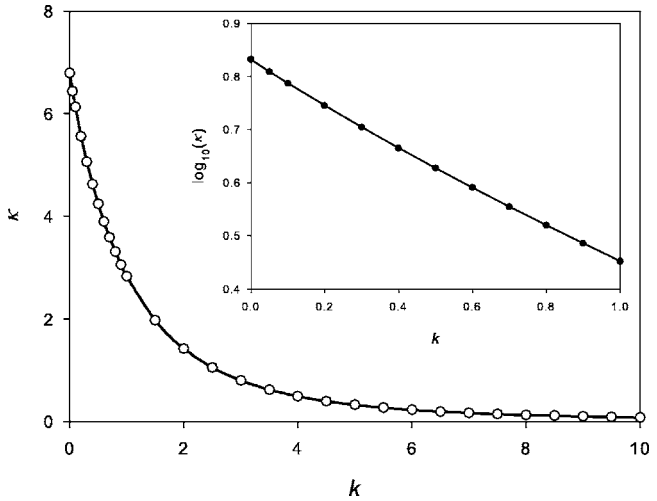

FIG. 16. The dependence of the thermal conduction $\varkappa$ on the parameter k, lattice interaction with boundaries. $N=50$, averaging over $M=500$ samples. Inset: the same dependence for $0\leqslant k\leqslant 1.0$ in semilogarithmic scale, i.e., $\log_{10}\varkappa\propto k$.

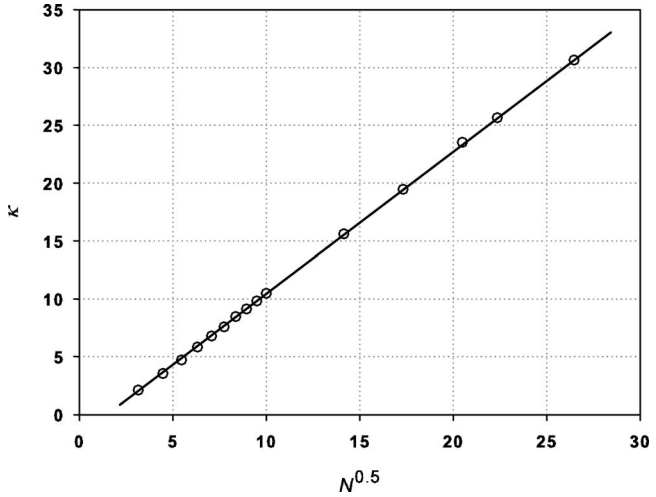

FIG. 17. The dependence of heat conduction $\varkappa$ the number N of particles in the lattice ($10\leqslant N\leqslant 700$). Free boundaries, averaging over $M=100$ samples.

It will be highly desirable to construct an "ideal" thermostat where the results of thermal conduction would not depend on parameters of thermostat. The Langevin thermostat has two parameters: the number of Langevin particles and the damping coefficient γ.

We consider now a lattice consisting of N particles interacting with N_T Langevin particles, simulating the thermostat, and attached to both ends of the lattice.

We hope that the physically reasonable limit can be obtained by the following sequence of limiting transitions: initially the size of thermostat $N_T\to\infty$, then the damping $\gamma\to 0$. The final limiting transition is $N\to\infty$.

We have chosen the simplest thermostat, the harmonic lattice of unit masses, and two methods are suggested to find the limiting value of thermal conduction with the increase of the thermostat size N_T. It turns out that the thermal conduction tends to the asymptotic value, approaching it exponentially with the increase of N_T. This is valid for rather small values of $\gamma\lesssim 0.5$. In Fig. 18 the dependence of thermal conduction $\varkappa$ on the number of Langevin particles N_T attached to both ends (at $\gamma=0.02$) is shown. The inset in Fig. 18 demonstrates the exponential decay of the difference $\varkappa(\infty)-\varkappa(N_T)$ with the growth of N_T.

The second method is the generalization of expression (34): for left Langevin sources,

$$J=\sum_{j=1}^{N_T}\frac{\gamma}{m(j)}[1-T(j)] \tag{38a}$$

and for right Langevin sources,

$$J=\sum_{j=N_T+N+1}^{2N_T+N}\frac{\gamma}{m(j)}T(j), \tag{38b}$$

where j numerates the Langevin particles, N is the number of "free" harmonic particles, and N_T is the number of Langevin particles equal for left and right ends. The addictiveness of the contribution from every Langevin sources to the total

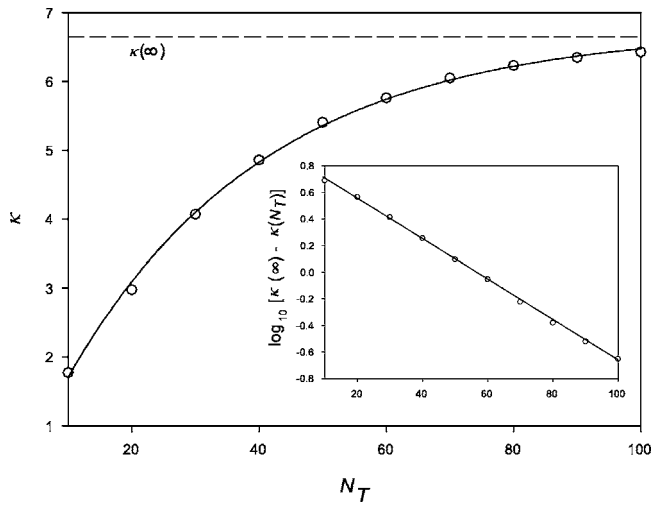

FIG. 18. The dependence of the thermal conduction $\varkappa$ the number N_T of the Langevin particles. $N=50$, averaging over $M=100$ samples, $\gamma=0.02$. $\varkappa(\infty)$ is the true asymptotic value at $N_T\to\infty$. Inset: the exponential approaching to the asymptotic value $\varkappa(\infty)$ with the increasing of the number of Langevin particles N_T.

heat flow is obvious from (38). Without the loss of generality we set the temperatures of all left Langevin sources to 1, and right sources to 0, i.e., $T_{Lg}(j)=1$ for $j=1,2,\ldots,N_T$ and $T_{Lg}(j)=0$ for $j=N+N_T+1,N+N_T+2,\ldots,N+2N_T$.

We found that at the right "cold" end the actual temperature inside the Langevin thermostat decreases exponentially with the number ℓ ($\ell=N+N_T+j$) of the Langevin particle counted from the Nth harmonic particle to the right (see Fig. 19).

An important property consists in the fact that the slopes of both approximating lines do not depend on the size of the Langevin thermostat, i.e., the slope in the dependence

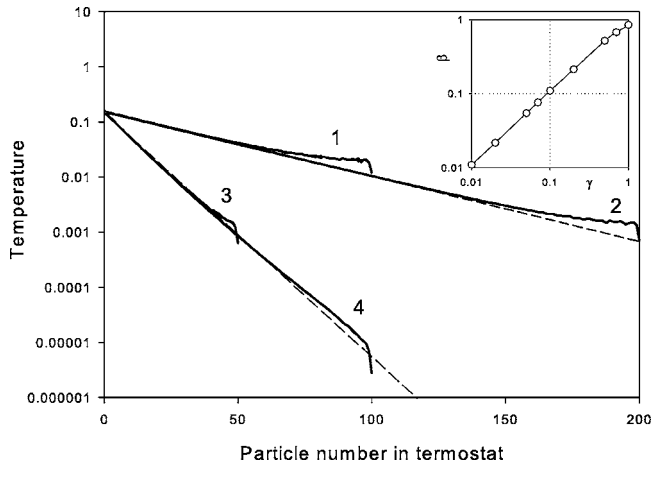

FIG. 19. The dependencies of the temperatures inside the right thermostat on the number of particles in the Langevin reservoir. 1, two almost indistinguishable curves for two samples with $N_T=100$ and $\gamma=0.25$; 2, the same as "1" for $N_T=200$; 3, two almost indistinguishable curves for two samples with $N_T=50$ and $\gamma=1$; 4, the same as "3" for $N_T=100$. $N=100$ in all cases. Dashed lines, linear approximations in semilogarithmic coordinates. Inset: the dependence of parameter β (see the text) on γ.

$\ln[T(\ell)]$ vs ℓ is independent on N_T. The slopes are also almost independent on the sample (fluctuations are $<2\%$). An index β in the dependence $T(\ell)=T(1)\exp(-\beta\ell)$ is proportional to γ and $\beta\simeq 1.09\gamma$ (see the inset in Fig. 19). Thus, (38b) is nothing else than the geometrical progression.

The limiting transition N_T can be made by computing the sum of geometrical progression in (38b). In the limit of small γ one can get that the value of thermal conduction is

$$J=\lim_{\gamma\to 0}\frac{\gamma}{\beta}T(1), \tag{39}$$

where "1" is the first particle in the Langevin thermostat with actual (nonLangevenian) temperature $T(1)$.

The existence of such a simple relation (39) opens the possibility for the computation of the thermal conduction in very large systems. The reason is that the computation of temperature $T(1)$, and, hence, the heat flow, becomes the much easier mathematical problem: it is necessary to find the eigenvalues of tridiagonal matrix without damping.

For the solving of the next problem (finding the thermodynamical limit $N\to\infty$) it is necessary to find the dependence of γ/β in (39) on the number of particles N. Our estimations show that $\lim_{N\to\infty}\gamma/\beta\sim 1.3$.

Thus, the computation of thermal conduction in very long lattices ($N>10^5$) is reduced to the following steps: first, one should be convinced in the final limit of $\lim_{\gamma\to 0}\gamma/\beta$ and find this limit, second, one should calculate the temperature $T(1)$ of the first Langevin particle in the thermostat. It can be done by finding the eigenvalues of the tridiagonal matrix of the dimensionality $(N+2N_T)\times(N+2N_T)$ a rather simple computational problem even for very large matrices. And finally one should solve the problem on the dependence of the temperature $T(1)$ on the thermostat size.

V. CONCLUSION

In this conclusion we briefly summarize our results. The mass-disordered lattice of particles interacting via harmonic forces with the Langevin thermostat was thoroughly investigated. We analyzed the dynamics, kinetics, and the thermal conduction in this model. There were two mathematically accurate methods developed which allowed us to increase the number of particles in the lattice up to $N=5000$, where the exact results can be obtained. Both methods are based on the equations for the correlation functions.

The considered model has highly localized vibrational modes with great relaxation times, and we have shown that these times increase exponentially with the number of particles in the lattice. The method was developed which allows us to calculate the relaxation times as large as $\gtrsim 10^{300}$. We have proved that the stationary state is unique.

The thermal conduction has the nontrivial behavior on N with the maximum at $N\sim 300$. For $N<300$ the dependence is $\propto\ln N$. For $N>300$ the asymptotic for the thermal conduction is $\varkappa\propto N^{-\alpha}$, where for $\gamma=1$ in Langevin forces, the exponent $\alpha\sim 0.27$. Lattices with a greater number of particles should be considered for the more accurate calculation of index α. We also demonstrated that $\varkappa$ is not the self-averaging value.

The stationary heat flow achieves its stationary value much faster compared to the achievement of stationary temperature profile, as the localized modes do not contribute to the thermal conduction. The computation of the heat flow demands much less efforts compared to the calculations of the stationary temperature profile.

An influence of parameter values was also thoroughly analyzed. We showed that the thermal conduction tends to zero in both limits: $\gamma \to 0$ and $\gamma \to \infty$. The dependence of $\varkappa$ vs γ is linear at small values of γ in accordance with [1].

Accurate results were obtained for the dependence of thermal conduction on the parameter of interaction with substrate, g. $\varkappa$ decreases exponentially with the growth of parameter g at a fixed number of particles in the lattice. Boundary conditions with the varying parameter k of the interaction with walls were also considered. The exponential decrease of the thermal conduction with the growth of parameter k was found.

A mass-disordered harmonic lattice is a nonphysical system in the sense that the computed values (heat flow, temperature profile, and the thermal conduction) are extremely sensitive to the values of parameter γ and number of particles N_T in the Langevin thermostat. Our goal was to construct a heat reservoir, where results would not depend on these parameters. We found that the true thermostat should consist of a large number of particles with very small damping, i.e., $N_T \to \infty$ and $\gamma \to 0$. It turned out that there is a simple method on how to find these limiting transitions. First, the temperatures in the Langevin thermostat decrease exponentially with parameter β with the number of Langevin particles. It allows us to use very simple expressions to calculate the limit $N_T \to \infty$. Second, there is a linear relation connecting parameters β and γ, and it allows us to get the next limiting transition $\gamma \to 0$. Thus, the suggested approach opens a possibility to calculate the thermal conduction of a very long ($N > 10^5$) lattice. Recall that everything stated above is valid only for the disordered harmonic lattices with the Langevin thermostat.

Some details of computations are presented in Appendixes A–C.

ACKNOWLEDGMENTS

This work was supported by the RFBR (Projects Nos. 04-03-32119 and 04-02-17306), and the Program of Presidium of Russian Academy of Sciences "Fundamental problems of physics and chemistry of nanosized systems and nanomaterials." The authors are indebted to L. I. Manevich and A. V. Savin (Institute of Chemical Physics, RAS, Moscow) for helpful comments.

APPENDIX A: CALCULATION OF EXPANSION COEFFICIENTS IN Eq. (29)

For the practical usage of Eq. (29) it is necessary to calculate sets of complex eigenvalues $\{\lambda_k\}$, eigenvectors $\{\boldsymbol{Q}_k\}$, and expansion coefficients $\{c_k\}$.

1. Eigenvalues and eigenvectors

At the numerical diagonalization of non-Hermitian matrix $\hat{A}$ (10) two sets of values are calculated simultaneously: imaginary eigenvalues ω_k and real inverse relaxation times $1/\tau_k$.

The double-precision numbers represented on the computer is limited by 14 digits. Therefore, if $\omega_k \sim 1$, then the precision in the calculation of $1/\tau_k$ cannot exceed 10^{-14}, i.e., the exact calculation of relaxation times is limited by $t \lesssim 10^{14}$ (which is nevertheless several orders of magnitude larger compared to the direct MD methods where times are limited by $t \lesssim 10^8 - 10^9$).

In an attempt to use (29) directly, the major problem is associated with the case of complex-conjugated roots when $\lambda_{k_1} = \lambda^*_{k_2}$, which could be a very small number equal to $-2/\tau_k$ for highly localized states.

a. Increasing of the accuracy of the relaxation time calculation

Below for definiteness we consider the particular case when Langevin sources act on two extreme particles of the lattice, the first and the Nth. We also set $\gamma(1) = \gamma(N) = \gamma$. As this takes place, there are only two terms in summation over p in (29): with $p=1$ and $p=N$.

The order of precision of relaxation time computation can be doubled. Namely, from the equation $\hat{A}\boldsymbol{Q} = \lambda \boldsymbol{Q}$ (24), rewritten in coordinate representation for the kth vibrational state, it follows:

$$m(i)\bar{x}_k(i)\lambda_k^2 = \bar{x}_k(i-1) - 2\bar{x}_k(i) + \bar{x}_k(i+1),$$

$$i = 2,3,\ldots,N-1, \tag{A1}$$

and two terms $-\gamma\lambda_k\bar{x}_k(i)$ (for $i=1$ and $i=N$) should be added to the rhs of (A1).

From this equation one can get (multiplying by complex conjugated, summing and dividing real and imaginary parts) an expression

$$\frac{1}{\tau_k} = -\gamma \frac{|\bar{x}_k(1)|^2 + |\bar{x}_k(N)|^2}{2\sum_{i=1}^{N} m(i)|\bar{x}_k(i)|^2}. \tag{A2}$$

There stands the value of the order of unity in the denominator (as the eigenvectors are normalized to unity). Then, if the eigenvector (more precisely, amplitudes of the kth vibrational states) is known with the precision $\sim 10^{-14}$, then the inverse relaxation times can be calculated with the precision $\sim 10^{-28}$. It means that the usage of a "double precision" number representation allows us to compute the dynamics of disordered systems for times $t \lesssim 10^{28}$, many orders of magnitude larger than is possible in the MD simulations.

Note that expression (A2) is sufficient to calculate the heat flows and temperatures at the lattice ends. Really, though this expression cannot give the correct values of τ_k for highly localized states [as their boundary values $\bar{x}_k(1)$ and $\bar{x}_k(N)$ cannot be calculated with the necessary level of accuracy], these highly localized states give negligible contributions to the heat flows.

b. Increasing the range of relaxation times up to $\tau \gtrsim 10^{300}$

We are interested now in highly localized states with great relaxation times, and our goal is to accurately estimate the temperature profile. We know an approximation to the eigenvector $\boldsymbol{Q}_k$ and eigenvalue λ_k for the kth localized state. Practically one can consider λ_k a purely imaginary value as its real part is a very small value. It is necessary to find a very small amplitude of $\bar{x}_k(1)$ and substitute it in (A2), keeping in mind that we construct the eigenvector with accurate values at the lattice ends. To do this we use Eq. (A1), which is nothing other than the recurrent relation for $\bar{x}_k(i)$.

Let us start from the initial boundary condition $\bar{x}_k(0)=0$, $\bar{x}_k(1)=1$ for some kth vibrational mode with known eigenvalue λ_k (an arbitrary initial condition can be chosen). Then recurrent procedure (A1) continues successfully until the largest amplitude $\bar{x}_k(L)$ at some particle L is reached.

After that this procedure repeats from the right side of the lattice and continues to the left until the same Lth particle is reached. Then both ("left" and "right") solutions are joined at the Lth particle, and the solution is normalized to unity. Finally one gets the eigenvector $\bar{\boldsymbol{x}}_k$ with excellent accuracy and the expression (A2) allows us to calculate very large relaxation times.

The greatest values of τ are $\lesssim 10^{300}$ (largest number available on PC with double precision).

2. Expansion coefficients c_k

The next problem is to find the expansion coefficients c_k in (29) with necessary accuracy. These values can be approximately estimated as $c_k \sim \bar{x}_k(1)$ and, as was shown above, $\bar{x}_k(1)$ can have extremely small values. Thus, because of limited accuracy of numerical calculations, direct solving of the linear system (28) is incorrect as the corresponding matrix $\hat{G}$ is ill defined.

It is reasonable to define the matrix "quality" through the matrix condition number as $\mathrm{cond}(\hat{G})=\|\hat{G}\|*\|\hat{G}^{-1}\|$, and $\|\hat{G}\|$ means some norm of a matrix. Practically it is more convenient to use the $\mathrm{rcond}(\hat{G})=1/\mathrm{cond}(\hat{G})$. If $\mathrm{rcond}(\hat{G})\sim 1$ then matrix $\hat{G}$ is well defined; and $\mathrm{rcond}(\hat{G})\ll 1$ in the opposite case.

If Eq. (28) is used directly then $\mathrm{rcond}(\hat{G})$ are 4.9×10^{-3}, 1.4×10^{-3}, $\sim10^{-6}$, and $\sim10^{-19}$ for $N=100$, 300, 500, and 1100 particles in the lattice. Thus, numerical accuracy catastrophically fails with the increasing number of particles.

We suggest a method which improves the accuracy of the calculation of expansion coefficients. Consider Eq. (28) once more

$$\sum_{k_1=1}^{2N} c_{k_1} Q_{k_1}(i) = \delta_{i1}. \tag{A3}$$

Our aim is to derive a more accurate equation for coefficients c_k. Let us introduce a symmetric matrix $B(k_1,k_2)$ which is the scalar product of eigenvectors $|\boldsymbol{Q}_{k_1}\rangle$ and $|\boldsymbol{Q}_{k_2}\rangle$ weighted by mass distribution $\hat{M}$ (hereafter we use "quantum" notations for vector/matrix operations)

$$B(k_1,k_2) = \left\langle \boldsymbol{Q}_{k_1} \left| \begin{pmatrix} \hat{M} & \hat{0} \\ \hat{0} & \hat{M} \end{pmatrix} \right| \boldsymbol{Q}_{k_2} \right\rangle. \tag{A4}$$

Later we shall demonstrate that the matrix (A4) is defined much better than the matrix (28). Equation (A3) for coefficients c_k can be rewritten as

$$\sum_{k_2=1}^{2N} B(k_1,k_2) c_{k_2} = m(1) Q_{k_1}(1). \tag{A5}$$

As the eigenvector satisfies the relation $|\boldsymbol{Q}_k\rangle=\{\lambda_k|\bar{\boldsymbol{x}}_k\rangle, |\bar{\boldsymbol{x}}_k\rangle\}$, one gets

$$B(k_1,k_2) = (1+\lambda_{k_1}\lambda_{k_2})\langle \boldsymbol{x}_{k_1}|\hat{M}|\boldsymbol{x}_{k_2}\rangle. \tag{A6}$$

Now we need to calculate the scalar product $\langle \boldsymbol{x}_{k_1}|\hat{M}|\boldsymbol{x}_{k_2}\rangle$. The immediate summation in an attempt to calculate this expression results in bad accuracy and we suggest a more accurate method for its calculation.

Write two equations (25) for different modes k_1 and k_2

$$\lambda_{k_1}^2|\bar{\mathbf{x}}_{k_1}\rangle = -\hat{U}|\bar{\mathbf{x}}_{k_1}\rangle - \lambda_{k_1}\hat{\Gamma}|\bar{\mathbf{x}}_{k_1}\rangle,$$

$$\lambda_{k_2}^2|\bar{\mathbf{x}}_{k_2}\rangle = -\hat{U}|\bar{\mathbf{x}}_{k_2}\rangle - \lambda_{k_2}\hat{\Gamma}|\bar{\mathbf{x}}_{k_2}\rangle. \tag{A7}$$

Multiply (from the left) first by $\langle \mathbf{x}_{k_2}|\hat{M}|$ and second by $\langle \mathbf{x}_{k_1}|\hat{M}|$ and subtract the first result from the second one. After simple calculus one gets the necessary expression for the matrix $B(k_1,k_2)$

$$B(k_1,k_2) = -(1+\lambda_{k_1}\lambda_{k_2})\frac{\langle \bar{\mathbf{x}}_{k_1}|\hat{\Gamma}|\bar{\mathbf{x}}_{k_2}\rangle}{\lambda_{k_1}+\lambda_{k_2}}. \tag{A8}$$

Matrix $\hat{B}$, calculated according to (A8), is defined much better. Its matrix condition numbers are 3.02×10^{-4}, 3.27×10^{-5}, 1.31×10^{-5}, 1.16×10^{-5} for $N=100, 300, 500, 1100$. Though $\mathrm{rcond}(\hat{B})$ are rather far from unity, $\mathrm{rcond}(\hat{B})$ does not depend on the number of particles. In the limit $\gamma\to0$ matrix $\langle \bar{\mathbf{x}}_{k_1}|\hat{M}|\bar{\mathbf{x}}_{k_2}\rangle$ is exactly the unit matrix as the eigenvectors are orthogonal with the weight $\hat{M}$.

An advantage of the calculations of the expansion coefficients c_k according to (A5) with matrix $B(k_1,k_2)$ defined by (A8) as compared with (28) is illustrated in Fig. 20. One can see that the improved method of this section gives results coinciding with theoretical predictions. Results obtained using (28) become much worse with the increasing number of particles N in the lattice.

APPENDIX B: PERTURBATION THEORY FOR FINDING EIGENVALUES AND EIGENVECTORS

The numerical solution of Eq. (24) for finding the eigenvalues and eigenvectors is a very "expensive" operation (in the sense of necessary computation time and memory). We suggest the method essentially accelerates this procedure.

For more easier perceiving we omit the subscript numerating the eigenvalues and eigenvectors, and make the re-

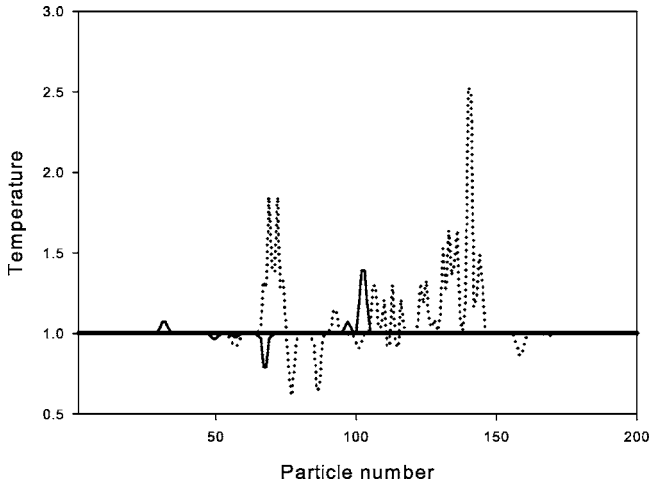

FIG. 20. The comparison of the temperature profiles for the lattices with $N=150$ (thin solid line), $N=200$ (dotted line) particles with equal temperatures of the Langevin sources $T_{\mathrm{Lg}}(1)=T_{\mathrm{Lg}}(N)=1$, calculated according to (28). The thick solid line is the exact result $[T(i)=1]$ and the expansion coefficients were calculated according to (A5).

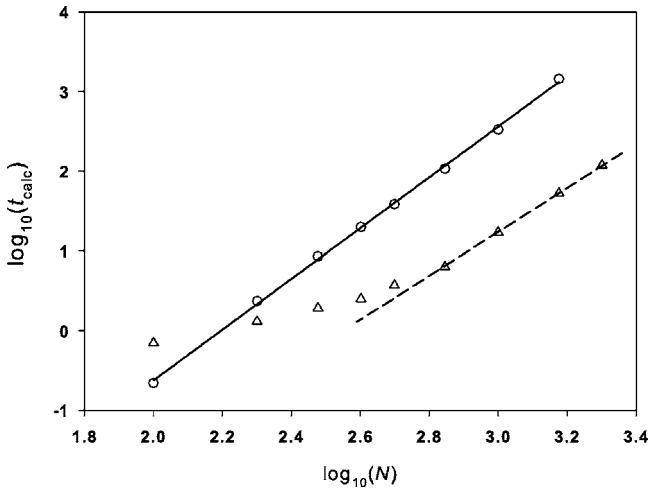

FIG. 21. Comparison of calculation times t_{calc} for lattices with $N=100-2000$. Empty circles, times of calculation in seconds using Eq. (24). Solid line, approximation by $t_{\mathrm{calc}}=10^{-7}N^{3.2}$ sec. Triangles, times of calculation in seconds by the method described in Appendix B with approximation $t_{\mathrm{calc}}=10^{-7.14}N^{2.8}$ sec. For large lattices the gain is more than 30 times. Computations were performed using a PC (3000 MHz).

placement $|\hat{M}^{-1/2}|\bar{x}\rangle \rightarrow |\bar{x}\rangle$. Then Eq. (25) will have the form

$$\lambda^2|\boldsymbol{x}\rangle = -|\hat{\tilde{U}}|\boldsymbol{x}\rangle - \lambda|\hat{\Gamma}|\boldsymbol{x}\rangle, \tag{B1}$$

where $\hat{\tilde{U}}=\langle\hat{M}^{-1/2}|\hat{U}|\hat{M}^{-1/2}\rangle$. As the zeroth approximation we chose Eq. (B1), where the term with damping $\hat{\Gamma}$ is omitted,

$$(\lambda^0)^2|\boldsymbol{x}^0\rangle = -|\hat{\tilde{U}}|\boldsymbol{x}^0\rangle, \tag{B2}$$

where $|\boldsymbol{x}^0\rangle$ and λ^0 are zeroth approximations. Note that numerical procedure (B2) is very fast as it solves the tridiagonal matrix. Note also that the Rayleigh-Schrödinger perturbation theory is not applicable in the considered case because of the semidegeneracy of eigenvalues (for large lattices eigenvalues lie very close).

We generalized the known method of back iterations with the shift developed for the linear eigenvalue problems $\hat{A}x=\lambda x$ for the case of the quadratic in the λ problem (B2).

The iteration procedure is the following. Choose random vector $|\boldsymbol{\zeta}\rangle$ and on the nth iteration step for the known eigenvalue λ^n the next approximation for the eigenvector $|\boldsymbol{x}^{n+1}\rangle$ is found as the solution of the following linear system:

$$(-\hat{\tilde{U}} - \lambda^n\hat{\Gamma} - (\lambda^n)^2\hat{I})|\boldsymbol{x}^{n+1}\rangle = |\boldsymbol{\zeta}\rangle. \tag{B3}$$

In an assumption that the eigenvectors are orthonormalized, we get the next approximation for the eigenvalue λ^{n+1}

$$(\lambda^{n+1})^2 = \langle\boldsymbol{x}^{n+1}| - \hat{\tilde{U}} - \lambda^n\hat{\Gamma}|\boldsymbol{x}^{n+1}\rangle. \tag{B4}$$

But it turns out that the convergence of the suggested method is too slow. We suggest an improved approach.

Multiplying unperturbed Eq. (B2) by $\langle\mathbf{x}^n|$ and Eq. (B1) by $\langle\mathbf{x}^0|$, substracting the results from each other, and taking into account the symmetry of matrix $\hat{\tilde{U}}$, one gets the square equation for the eigenvalue λ^{n+1}

$$(\lambda^{n+1})^2 + \lambda^{n+1}\frac{\langle\mathbf{x}^0|\hat{\Gamma}|\mathbf{x}^n\rangle}{\langle\mathbf{x}^0|\mathbf{x}^n\rangle} - (\lambda^0)^2 = 0, \tag{B5}$$

and the root with definite sign (say, positive) should be chosen in every case. This method allows us to get new eigenvalues and eigenvectors, and replaces the described above recurrent procedure (B4).

The method described above was completed by the Arnoldi method, based on the Krylov subspace [34], allowing us to compute only a few eigenvalues, which belong to one or another part of the spectrum, e.g., eigenvalues with largest (smallest) real (imaginary) parts. Note that the Arnoldi method is the generalization of the Lanczosi method for unsymmetrical matrices.

As we are mainly interested in eigenvalues with least real parts, then the Arnoldi method was adjusted to search usually ~ 10 lowest eigenstates.

Additional reduction of computational time was achieved by the fact that for $N \gtrsim 1000$ the total number of vibrational states giving contribution to thermal conduction constitutes approximately only one-third from the total number of vibrational states. It allows us to considerably reduce the dimensionality of matrix $B(k_1,k_2)$ at solving the linear system of the equation for c_k.

The comparison of times of computation by solving Eqs. (24) and by methods described in this appendix is shown in Fig. 21. We have compared the method of this appendix with exact results, and found that the total error does not exceed 2% because of some numbers of unfound states.

APPENDIX C: TEMPERATURE PROFILE IN THE LIMIT $\gamma \to 0$

Here we shall demonstrate how our results (29) are transformed in the limit $\gamma \to 0$. We are planning to obtain the results of works [37,38], where this limit was studied.

For clarity we again consider the case of only one Langevin particle with $T_{\mathrm{Lg}}(1)=1$. As we consider the stationary state ($t \to \infty$), time variables are omitted. The stationary temperature profile $[T(i) \equiv m(i)\langle v^2(i)\rangle]$ has the form

$$T(i) = -\frac{2T_{\mathrm{Lg}}(1)}{m^2(1)} m(i) \sum_{k_1,k_2=1}^{2N} \frac{\gamma}{\lambda_{k_1}+\lambda_{k_2}} Q_{k_1}(i) Q_{k_2}(i) c_{k_1} c_{k_2}. \tag{C1}$$

We are planning to make the limiting transition $\gamma \to 0$. As the expression (C1) contains many terms and all of them depend on γ, they will be considered separately.

(1) *The limit of* $|\boldsymbol{Q}_k\rangle$ *at* $\gamma \to 0$. At $\gamma \to 0$ the equation for $|\bar{\boldsymbol{x}}_k\rangle$ (25) transforms to the equation for eigenvalues of symmetrical and real matrix $\hat{U}$

$$\lambda_k^2 \hat{M} |\bar{\boldsymbol{x}}_k\rangle = -\hat{U} |\bar{\boldsymbol{x}}_k\rangle, \tag{C2}$$

and real eigenvectors $|\bar{\boldsymbol{x}}_k\rangle$ are orthonormal with weight $\hat{M}$

$$\langle \bar{\boldsymbol{x}}_{k_1} | \hat{M} | \bar{\boldsymbol{x}}_{k_2} \rangle \equiv \sum_i \bar{x}_{k_1}(i) m(i) \bar{x}_{k_2}(i) = \delta_{k_1 k_2}. \tag{C3}$$

Note, that in (C2) $\lambda^2 < 0$. It also means that there are two complex conjugated vectors $|\boldsymbol{Q}_k\rangle$ and $|\boldsymbol{Q}_k^*\rangle$ for every real vector $|\bar{\boldsymbol{x}}_k\rangle$

$$|\boldsymbol{Q}_k\rangle = (i\omega_k |\bar{\boldsymbol{x}}_k\rangle, |\bar{\boldsymbol{x}}_k\rangle), \quad |\boldsymbol{Q}_k^*\rangle = (-i\omega_k |\bar{\boldsymbol{x}}_k\rangle, |\bar{\boldsymbol{x}}_k\rangle), \tag{C4}$$

and $\omega_k = \sqrt{-\lambda_k^2}$.

It is convenient to rearrange $2N$ vectors $|\boldsymbol{Q}_k\rangle$ in such a way that last N vectors be complex conjugated to first N vectors. Let us define matrix $\hat{Q}$, constructed in such a way that the matrix $\hat{Q}$ with rearranged vectors $|\boldsymbol{Q}_k\rangle$ has the form

$$\hat{Q} = \begin{pmatrix} i\hat{\bar{X}}\hat{\Omega} & -i\hat{\bar{X}}\hat{\Omega} \\ \hat{\bar{X}} & \hat{\bar{X}} \end{pmatrix}, \tag{C5}$$

where the $N \times N$ matrices $\Omega(i,k)$ and $\bar{X}(i,k)$ are equal to $\omega_k \delta_{ik}$ and $\bar{x}_k(i)$. In the limit $\gamma \to 0$ vectors $|\boldsymbol{Q}_k\rangle$ are defined by (C4), and vectors $|\bar{\boldsymbol{x}}_k\rangle$ by (C2).

(2) *The limit of* c_k *at* $\gamma \to 0$. Equation (28) for coefficients c_k can be rewritten in the matrix form

$$\begin{pmatrix} i\hat{\bar{X}}\hat{\Omega} & -i\hat{\bar{X}}\hat{\Omega} \\ \hat{\bar{X}} & \hat{\bar{X}} \end{pmatrix} \begin{pmatrix} c^1 \\ c^2 \end{pmatrix} = \begin{pmatrix} 1 \\ 0 \\ \cdots \\ 0 \end{pmatrix}, \tag{C6}$$

where for the convenience we denoted $c_k^1 \equiv c_k, k \leqslant N$, and $c_k^2 \equiv c_k, k > N$. We have $\boldsymbol{c}^2 = -\boldsymbol{c}^1$ [it follows from the equation $\Sigma_k \bar{\boldsymbol{x}}_k (c_k^1 + c_k^2) = 0$]. Then the equation for $\boldsymbol{c}^1$ is

$$\sum_{k=1}^{N} \bar{x}_k(i)(2i\omega_k c_k^1) = \delta_{i1}. \tag{C7}$$

Multiplying this expression by vector $|\bar{\boldsymbol{x}}_k\rangle$ (with weight $\hat{M}$) and using the orthonormality of vectors $|\bar{\boldsymbol{x}}_k\rangle$ [see (C3)], one gets

$$c_k = \frac{m(1)}{2i\omega_k} \bar{x}_k(1), \tag{C8}$$

and our previous suggestion that $c_k \sim \bar{x}_k(1)$ is supported.

(3) *The limit of fraction* $\gamma/(\lambda_{k_1}+\lambda_{k_2})$ *at* $\gamma \to 0$. In the limit $\gamma \to 0$ the imaginary parts of eigenvalues (ω_k) have finite values defined by (C2). But the real parts ($1/\tau_k$) tends to zero ($\propto \gamma$). Therefore, it is obvious that the nonzero answer in the limit $\gamma \to 0$ could be obtained only if $\lambda_{k_1} = \lambda_{k_2}^*$. Then in the denominator there stands the value $\lambda_{k_1} + \lambda_{k_2}^* = 2\,\mathrm{Re}\,\lambda_{k_1}$ and this value is of the order γ.

From the equation for real parts of eigenvalues (A2) and taking into account that $\langle \bar{x}_k | \hat{M} | \bar{x}_k \rangle = \hat{1}$ one gets

$$\gamma/(\lambda_{k_1}+\lambda_{k_2}) \to -[\bar{x}_{k_1}^2(1) + \bar{x}_{k_2}^2(N)]^{-1}. \tag{C9}$$

Expression (C9) is accurate if k_1 and k_2 correspond to complex conjugated vectors, otherwise this limit (at $\gamma \to 0$) is null.

(4) *And the final step*. In the double summation in (C1) for $T(i)$ there will "survive" only terms with $\lambda_{k_1} = \lambda_{k_2}^*$ and the sum becomes over one variable. In the expression (C1) for temperatures we (1) substitute the expression for fraction (C9), and (2) make transformation to the summation from 1 to N as complex conjugated values are met twice. As a result an additional multiplier "2" arises,

$$T(i) = \frac{4T_{\mathrm{Lg}}(1)}{m^2(1)} m(i) \sum_{k=1}^{N} \frac{|Q_k(i)|^2 |c_k|^2}{[\bar{x}_k^2(1) + \bar{x}_k^2(N)]}. \tag{C10}$$

Substituting expression (C8) for c_k in (C10), and expression for $Q_k(i) = i\omega_k \bar{x}_k(i)$; $i = 1, 2, \ldots, N$, we get

$$T(i) = T_{\mathrm{Lg}}(1) m(i) \sum_{k=1}^{N} \frac{\bar{x}_k^2(1)\bar{x}_k^2(i)}{\bar{x}_k^2(1) + \bar{x}_k^2(N)}. \tag{C11}$$

To get the result presented in [37,38], one should make the substitution $\sqrt{m(i)}\bar{x}_k(i) \to e_k(i)$.

[1] S. Lepri, R. Livi, and A. Politi, Phys. Rep. **377**, 1 (2003).
[2] F. Bonetto, J. L. Lebowitz, and L. Rey-Bellet, in *Mathematical Physics 2000*, edited by A. Fokas *et al.* (Imperial College Press, London, 2000), pp. 128–150.
[3] S. Lepri, R. Livi, and A. Politi, Phys. Rev. Lett. **78**, 1896 (1997).
[4] S. Lepri, R. Livi, and A. Politi, Europhys. Lett. **43**, 271 (1998).
[5] A. V. Savin, G. P. Tsironis, and A. V. Zolotaryuk, Phys. Rev. Lett. **88**, 154301 (2002).
[6] T. Hatano, Phys. Rev. E **59**, R1 (1999).
[7] A. Dhar, Phys. Rev. Lett. **86**, 3554 (2001).
[8] P. L. Garrido, P. I. Hurtado, and B. Nadrowski, Phys. Rev. Lett. **86**, 5486 (2001).
[9] C. Giardina, R. Livi, A. Politi, and M. Vassalli, Phys. Rev. Lett. **84**, 2144 (2000).
[10] O. V. Gendelman and A. V. Savin, Phys. Rev. Lett. **84**, 2381 (2000).
[11] L. Yang, P. Grassberg, e-print cond-mat/0306173.
[12] M. H. Ernst, Physica D **47**, 198 (1991).
[13] J.-S. Wang and B. Li., Phys. Rev. Lett. **92**, 074302 (2004).
[14] O. Narayan and S. Ramaswamy, Phys. Rev. Lett. **89**, 200601 (2002).
[15] A. Dhar, Phys. Rev. Lett. **86**, 5882 (2001).
[16] G. Zhang and B. Li, J. Chem. Phys. **123**, 014705 (2005).
[17] B. Li, J. Wang, L. Wang, and G. Zhang, Chaos **15**, 015121 (2005).
[18] D. Segal and A. Nitzan, J. Chem. Phys. **122**, 194704 (2005).
[19] G. Casati, Chaos **15**, 015120 (2005).
[20] M. Terrano, M. Peyrard, and G. Casati, Phys. Rev. Lett. **88**, 094302 (2002).
[21] B. Li, L. Wang, and G. Casati, Phys. Rev. Lett. **93**, 184301 (2002).
[22] S. Maruyama, in *Advances in Numerical Heat Transfer*, Vol. 2, (2000), edited by W. J. Minkowjcz and E. M. Sparrow (Taylor & Francis, New York, 2000), 189.
[23] S. Maruyama, Physica B **323**, 193 (2002).
[24] S. Maruyama, Microscale Thermophys. Eng. **7**, 41 (2003).
[25] J. X. Cao, X. H. Yan, Y. Xiao, Y. Tang, and J. W. Ding, Phys. Rev. B **67**, 045413 (2003).
[26] J. X. Cao, X. H. Yan, Y. Xiao, and J. W. Ding, Phys. Rev. B **69**, 073407 (2004).
[27] M. A. Osman and D. Srivastava, Nanotechnology **12**, 21 (2001).
[28] A. Cummings, M. Osman, D. Srivastava, and M. Menon, Phys. Rev. B **70**, 115405 (2004).
[29] G. Wu and J. Dong, Phys. Rev. B **71**, 115410 (2005).
[30] F. J. Dyson, Phys. Rev. **92**, 1331 (1953).
[31] M. Rich and W. M. Visscher, Phys. Rev. B **11**, 2164 (1975).
[32] R. Kubo, M. Toda, and N. Hashimitsume, *Statistical Physics II*, Springer Series in Solid State Sciences Vol. 31 (Springer, Berlin, 1991).
[33] P. J. Forrester, N. C. Snaith, and J. J. M. Verbaarschot, e-print cond-mat/0303207.
[34] D. C. Sorensen, SIAM J. Matrix Anal. Appl. **13**, 357 (1992).
[35] P. W. Anderson, Phys. Rev. **109**, 1492 (1958).
[36] N. Mott and W. Twose, Adv. Phys. **10**, 107 (1961).
[37] H. Matsuda and K. Ishii, Prog. Theor. Phys. **45**, 56 (1970).
[38] W. M. Visscher, Prog. Theor. Phys. **46**, 729 (1971).
[39] A. J. O'Connor and J. L. Lebowitz, J. Math. Phys. **15**, 692 (1974).
[40] A. Dhar, Phys. Rev. Lett. **87**, 069401 (2001).
[41] B. Li, H. Zhao, and B. Hu, Phys. Rev. Lett. **86**, 63 (2001).
[42] B. Li, H. Zhao, and B. Hu, Phys. Rev. Lett. **87**, 069402 (2001).